The Hrq1 helicase stimulates Pso2 translesion nuclease activity to promote DNA inter-strand crosslink repair

Cody M. Rogers[1], Chun-Ying Lee[2], Samuel Parkins[3], Nicholas J. Buehler[1], Sabine Wenzel[4], Francisco Martínez-Márquez[4], Yuichiro Takagi[4], Sua Myong[2], and Matthew L. Bochman[1,*]

[1] Molecular and Cellular Biochemistry Department, Indiana University, Bloomington, IN 47405, USA
[2] Department of Biophysics, Johns Hopkins University, Baltimore, MD 21218, USA
[3] Department of Biology, Johns Hopkins University, Baltimore, MD 21218, USA
[4] Department of Biochemistry and Molecular Biology, Indiana University School of Medicine, Indianapolis, IN 46202, USA

* To whom correspondence should be addressed. Tel: +1 812-856-2095; Fax: 812-856-5710; Email: bochman@indiana.edu

ABSTRACT

DNA inter-strand crosslink (ICL) repair requires a complicated network of DNA damage response pathways. Removal of these lesions is vital as they are physical barriers to essential DNA processes that require the separation of duplex DNA, such as replication and transcription. The Fanconi anemia (FA) pathway is the principle mechanism for ICL repair in metazoans and is coupled to replication (1). In *Saccharomyces cerevisiae*, a degenerate FA pathway is present, but ICLs are predominantly repaired by a pathway involving the Pso2 nuclease that is hypothesized to digest through the lesion to provide access for translesion polymerases (2). However, mechanistic details of this pathway are lacking, especially relative to FA. We recently identified the Hrq1 helicase, a homolog of the disease-linked RECQL4, as a novel component of Pso2-mediated ICL repair (3). Here, we show that Hrq1 stimulates the Pso2 nuclease in a mechanism that requires Hrq1 catalytic activity. Importantly, Pso2 alone has meagre translesion nuclease activity on an ICL-containing substrate, but digestion through the lesion dramatically increases in the presence of Hrq1. Stimulation of Pso2 nuclease activity is specific to eukaryotic RecQ4 subfamily helicases, and Hrq1 interacts with Pso2, likely through their N-termini. These results advance our understanding of FA-independent ICL repair and establish a role for the RecQ4 helicases in the repair of these dangerous lesions.

INTRODUCTION

DNA inter-strand crosslinks (ICLs) are covalent linkages between complementary DNA strands, and they act as physical barriers to essential DNA transactions like replication and transcription (4). Repair of these lesions is vital for cell survival, and 20-40 lesions are lethal to repair-deficient mammalian cells (5). For this reason, DNA damaging agents that cause ICLs are common chemotherapeutics, and upregulation of pathways that repair these lesions is a known source of chemotherapeutic resistance (4). To date, the most thoroughly studied ICL repair mechanism involves the Fanconi anemia (FA) pathway in which over 20 proteins are involved (6). The main mechanism for FA-dependent ICL repair is coupled to DNA replication. Briefly, the replisome stalls 20-40 nts from the ICL, which results in uncoupling of the replicative helicase MCM2-7 and DNA synthesis to within 1 nt of the lesion (1). Unhooking of the lesion is accomplished by a suite of nucleases that act in a context-

specific manner (reviewed in (7)). This results in a double-strand break (DSB), which is repaired by homologous recombination (HR). Subsequently, translesion polymerases replicate past the ICL, and nucleotide excision repair (NER) factors remove the remaining adducted nucleotide. However, it has also been shown that a large number of ICLs can be bypassed by an intact replisome in a traverse model in a FA-dependent manner (8). Variations of this mechanism are dependent on the context in which the ICL is identified, and the FA pathway only accounts for ICL repair during S-phase. Importantly, there are numerous ICL repair factors that do not fall within the FA complementation group, including proteins in the SAN1/SETX pathway (9), base excision repair-associated ICL repair (10,11), and the SNM1/Pso2 family nucleases (12). Taken together, ICL repair requires the complex coordination of multiple pathways that depend on the context of the lesion.

Of the three SNM1 proteins in humans (SNM1A, SNM1B (Apollo), and SNM1C (Artemis)), SNM1A is the most directly linked to ICL repair (12), though SNM1B has a role in ICL repair that is independent of SNM1A (2). The model for SNM1A in ICL repair starts with NER factors such as XPF-ERCC1 and FAN1 using their endonuclease activity to create a single-stranded (ss)DNA nick on either the 5′ side of the lesion or on both sides, though other nucleases have been implicated in this process (reviewed in (7)). SNM1A uses its 5′ → 3′ exonuclease activity to digest from the incision through the ICL, facilitating gap fill-in by translesion DNA polymerases (13). While SNM1A appears to play an important role in ICL repair in vertebrates, the FA pathway is the dominant mechanism for ICL repair. However, the *Saccharomyces cerevisiae* homolog of SNM1A, Pso2, is involved in the predominant pathway for ICL repair in yeast (3,14). Indeed, human SNM1A is able to suppress the sensitivity of *pso2Δ* cells to ICL damage (15). Similar to its human counterpart, Pso2 possesses 5′ → 3′ exonuclease activity (16), as well as structure-specific endonuclease activity (17). Currently, the mechanism for Pso2 ICL repair is unclear, but we recently identified the *S. cerevisiae* RECQL4 homolog, the Hrq1 helicase, as an additional component of Pso2-dependent ICL repair pathway (3).

The RecQ family helicases are conserved mediators of genome stability, with five family members encoded by the human genome (reviewed in (18)). Mutations in three of the human RecQ helicases (BLM, WRN, and RECQL4) are directly linked to diseases that clinically overlap in their predisposition to cancer and premature aging phenotypes. The involvement of RECQL4 in ICL repair is unclear (19), largely due to technical challenges associated with RECQL4 analysis. Since the identification of RecQ4 helicases in various fungal and plants species (20), new homologs have been identified in bacteria and archaea (21,22), making RECQL4 the only RecQ subfamily helicase conserved in all three domains of life. Recent work on the RECQL4 homologs in *Arabidopsis thaliana* (23) and *S. cerevisiae* (3,24), both called Hrq1, demonstrates that they are involved in ICL repair, similar to RECQL4 (25). Furthermore, Hrq1 appears to be a *bona fide* RECQL4 homolog *in vitro* and *in vivo*, making it a good model for RECQL4-mediated DNA repair (3,24,26). Hrq1 is currently the only known protein to work with Pso2 at the post-incision step of ICL repair, but its mechanism of action is unclear.

Here, we provide further evidence that Hrq1 functions alongside Pso2 to repair ICL lesions that vary in their DNA sequence preference and effect on DNA structure. *In vitro*, Hrq1 stimulates Pso2 nuclease activity in a reaction that requires Hrq1 catalytic activity, and this phenomenon is specific to

RecQ4 subfamily helicases. Pso2 stalling at a site-specific ICL can be overcome in the presence of Hrq1. Finally, we demonstrate that the Pso2 N-terminus is an autoinhibitory domain that likely acts as the interaction platform for Hrq1-mediated nuclease stimulation. These data support the direct role of RecQ4 family helicases in ICL processing and provide mechanistic insight into the Pso2-dependent ICL repair pathway.

MATERIAL AND METHODS

Reagents, nucleotides, and oligonucleotides

γ[^{32}P]-ATP and α[^{32}P]-dCTP were purchased from PerkinElmer (Waltham, MA). Unlabelled ATP was purchased from DOT Scientific (Burton, MI), and all oligonucleotides were synthesized by IDT (Coralville, IA) and are listed in Supplemental Table 1.

DNA inter-strand crosslinker sensitivity analysis

The sensitivity of *S. cerevisiae* mutants to DNA damaging agents was analysed as described (3). Briefly, cells were grown overnight in 1% yeast extract, 2% peptone, and 2% dextrose (YPD) medium with aeration and diluted to an optical density at 660 nm (OD_{660}) of 1 in sterile water. Cells were then serially diluted 10-fold to 10^{-4}, and 5 µL of each dilution was spotted onto YPD plates lacking or containing the indicated drug. For mitomycin C (MMC) and diepoxybutane (DEB), plates contained 50 µg/mL of the respective drug, unless otherwise indicated. Plates containing 20 µg/mL 8-methoxypsoralen (8-MOP) were treated with 365 nm UVA (Sylvania fluorescent lamp) in a dark box for 30 min after cells were spotted to activate the ICL reaction. Methyl methanesulfonate (MMS) was used at 0.03%. All plates were incubated in the dark for 2 days at 30°C and imaged on a flat-bed scanner. The strains were constructed in the wild type YPH499 background (*MATa, ura3-52, lys2-801_amber, ade2-101_ochre, trp1Δ63, his3Δ200, leu2Δ1*) (27) using standard methods.

Protein expression and purification

The *S. cerevisiae* Pso2 expression vector harbouring a C-terminal 6xHis-tag was kindly provided by Murray Junop (Schulich School of Medicine and Dentistry, Western University) (17). Pso2-6xHis was expressed in Rosetta 2(DE3) pLysS (Novagen) cells by growing cultures to an OD_{600} of 0.6 at 37°C followed by induction with 1 mM isopropyl β-D-1-thiogalactopyranoside for 4 h at 30°C. Cells were harvested by centrifugation at 5000 rpm for 10 min at 4°C, and the cell pellet was frozen at -80°C. The frozen cell mass was thawed in Resuspension Buffer (50 mM NaHEPES, pH 7, 50 mM NaCl, 5% glycerol, and 2 mM DTT) supplemented with fresh protease inhibitor mix and 20 µg/mL DNase I. Lysis was performed using several passes through a cell cracker, and the lysate was clarified by centrifugation at 14,000 rpm for 30 min at 4°C. Clarified lysate was loaded onto a gravity column containing 1 mL HIS-Select Nickel Affinity Gel (Sigma) pre-equilibrated with Resuspension Buffer. The column was washed with 5 column volumes (CVs) of Resuspension Buffer and 5 CVs of Resuspension Buffer supplemented with 5 mM ATP. Pso2 was eluted with Resuspension Buffer supplemented with 100 mM imidazole, and the Pso2-containing fractions were pooled. The eluate

was then loaded onto 1 mL HiTrap Heparin HP column (GE Healthcare) and washed with 10 CVs Heparin Buffer (50 mM NaHEPES, pH 7, 50 mM NaCl, 5% glycerol, and 2 mM DTT). Pso2 was eluted via a 20-CV linear salt gradient with Heparin Buffer from 50 mM to 1 M NaCl. Pooled Pso2 fractions were concentrated and buffer exchanged into storage buffer (25 mM NaHEPES, pH 7.6, 30% glycerol, 300 mM NaOAc pH 7.6, 25 mM NaCl, 5 mM MgOAc, 1 mM DTT, and 0.01% Tween-20). Pso2ΔN and the catalytically inactive Pso2-H611A mutant were purified identically to wild-type.

Expression and purification of Hrq1 and RECQL4 were described previously (3). Sgs1 was a generous gift from Hengyao Niu (Indiana University) and Petr Cejka (Università della Svizzera italiana).

Hrq1ΔN was purified similarly to the wild-type Hrq1 used in (24). Briefly, a plasmid harboring the 3xStrep-Hrq1ΔN-6xHis construct was transformed into Rosetta 2(DE3) pLysS cells and expressed overnight in autoinduction media (28). Cells were lysed in Hrq1ΔN Resuspension Buffer (50 mM NaHEPES,pH 8, 5% glycerol, 150 mM NaOAc, pH8, 5 mM MgOAc, and 0.05% Tween-20) as in the Pso2 purification, and clarified lysate was loaded onto a 1 mL StrepTrap column. The column was washed with 20 CVs Hrq1ΔN Resuspension Buffer supplemented with 600 mM NaOAc, followed by a wash with Hrq1ΔN Resuspension Buffer supplemented with 5 mM ATP. Protein was eluted in buffer containing 2.5 mM desthiobiotin. Protein-containing fractions were pooled and loaded onto a 0.5-mL His60 column. The column was washed with 10 CVs Hrq1ΔN Resuspension Buffer containing 10 mM imidazole, followed by a 1-CV wash each with buffer supplemented with 50 and 100 mM imidazole. Protein was eluted in Hrq1ΔN Resuspension Buffer supplemented with 500 mM imidazole and stored as for Pso2. *Mycobacterium smegmatis* SftH was purified identically. Further details concerning the construction of expression vectors and protein purification are available upon request.

Preparation of DNA substrates

The uncrosslinked double-stranded (ds)DNA substrate was prepared by annealing equimolar amounts of MB1614 to MB1461 in Annealing Buffer (20 mM Tris-HCl, pH 8, 4% glycerol, 0.1 mM EDTA, 40 µg/mL BSA, 10 mM DTT, and 10 mM MgOAc) overnight at 37°C (29) (Supplemental Table 1). Because Pso2 nuclease activity is greatly stimulated by a 5′-phosphate, only the digested strand (MB1614) was phosphorylated by IDT. The substrate was designed such that the digested strand is 6 nt shorter than the undigested strand to allow 3′ fill-in by Klenow Fragment (3′-5′ exo-; NEB) with α[^{32}P]-dCTP and cold dATP, dTTP, and dGTP for 30 min at 37°C. After labelling, cold dCTP was also added for another 30 min at 37°C to facilitate complete fill-in to yield a 30-bp blunt dsDNA. The nuclease substrate was separated from unincorporated dNTPs using an illustra ProbeQuant G-50 micro column (GE Healthcare) according to the manufacturer's instructions.

The ICL-containing substrate was prepared using spontaneous crosslink formation from an abasic site as previously reported (30). Oligonucleotides MB1599 and MB1600 were annealed by heating to 95°C for 5 min followed by slow cooling to room temperature overnight. The digested strand (MB1599) was 5′ phosphorylated as above and contained a deoxyuracil (dU) 7-nt from the 5′ end. The substrate

was then treated with 50 U of uracil DNA glycosylase (NEB) for 2 h at 37°C to form the abasic site. The DNA was phenol/chloroform extracted and precipitated with 10% 3 M NaOAc, pH 5.2, and five volumes of 100% ethanol. Precipitated DNA was stored at -20°C for 1 h and pelleted at 15,000 rpm for 30 min at 4°C. The supernatant was removed, and the pellet was washed twice with cold 80% ethanol. After the last wash was completely removed, the DNA was resuspended in 50 mM NaHEPES, pH 7, and 100 mM NaCl and stored in the dark for 5 days with gentle agitation to form the ICL. Once the crosslink was formed, the substrate was labelled with α[^{32}P]-dCTP as above. The DNA was heated at 95°C for 10 min to denature any uncrosslinked substrate, and the entire sample was loaded onto a 20% 19:1 acrylamide:bis-acrylamide 6 M urea denaturing gel and run in 1x TBE buffer (90 mM Tris-HCl pH 8.0, 90 mM boric acid, and 2 mM EDTA, pH 8.0) at 10 V/cm. The gel was exposed to classic blue autoradiography film to identify the slower migrating ICL-containing dsDNA, which was gel extracted into 0.5x TBE buffer overnight and precipitated as above. The crosslinked substrate was finally resuspended in H_2O.

To make forked DNA for helicase assays, the top strand (MB733) was 5′ labelled with γ[^{32}P]-ATP and T4 polynucleotide kinase (T4 PNK; NEB) for 1 h at 37°C and cleaned up with a G-50 micro column as above. Equimolar cold bottom strand (MB734) was incubated with labelled top strand overnight at 37°C in Annealing Buffer. Helicase assays using blunt dsDNA were performed with the undamaged nuclease assay substrate described above (MB1614 annealed to MB1461).

Gel-based nuclease assays

Nuclease assays were performed for 30 min at 30°C with the indicated protein concentration in Nuclease Buffer (20 mM Tris-acetate, pH 7.6, 50 mM NaOAc, pH 7.6, 7.5 mM MgOAc, and 0.01% Tween-20) with 1 nM labelled DNA substrate. For nuclease assays involving helicases, 5 mM ATP was also included unless stated otherwise. Reactions were stopped with the addition of Loading Dye (95% formamide and 0.02% bromophenol blue) and by heating at 95°C for 5 min. Reactions were loaded onto 20% 19:1 acrylamide:bis-acrylamide 6 M urea denaturing gels in 1x TBE buffer and run at 2400 V for 90 min. Gels were dried under vacuum, imaged using a Typhoon FLA 9500, and quantified using ImageQuant 5.2.

smFRET nuclease assays

Single molecule assays were performed by using a home-built prism type total internal reflection fluorescence (TIRF) microscope at room temperature (24 ± 1°C). The microscope setup, slide preparation, and DNA immobilization were performed as described (31). The experimental protocol and flow setup were slightly modified from a previously published method (32). The MB1621 DNA oligonucleotide was purchased from IDT with 5'-Cy3, 3'-biotin, and an internal amine modification (Supplementary Table 1). The amine modification was used for Cy5 labeling as described (33). The labelled oligonucleotide was annealed to MB1620 or MB1622 to make the ICL-containing or undamaged substrate, respectively. The abasic site crosslink was formed as above.

The buffer used for Pso2 nuclease activity measurement was prepared freshly by mixing an oxygen scavenging system (1 mg/mL glucose oxidase, 0.8% v/v glucose, ~10 mM Trolox, and 0.03 mg/mL catalase) before taking each single molecule image. A solid-state 532 nm laser was used for FRET measurement. Images were recorded with a time resolution of 100 ms and analysed by Matlab. FRET efficiency (E) was calculated by the equation:

$$E = \frac{I_A - r \cdot I_D}{I_D + I_A}$$

I_D and I_A are the intensities of Cy3 (donor) and Cy5 (acceptor). *r* is the correction factor for donor leakage, which is 0.15 for our system. Each FRET histogram was generated by collecting FRET values from at least 6000 molecules taken over 15~20 movies. The FRET histograms were fit with a Gaussian distribution function. For nuclease activity, 50 nM Pso2 and 150 nM Hrq1 (or Hrq1-K318A) were used in all of the experiments, and each reaction was terminated by 0.1% SDS treatment and flushed with TE (90 mM Tris-HCl, pH 8, and 2 mM EDTA, pH 8) to remove protein.

Protein-protein crosslinking

Disuccinimidyl sulfoxide (DSSO) was resuspended in DMSO to the desired concentration. Reactions contained 500 nM Hrq1, 500 or 100 nM Pso2, and a molar excess of DSSO as indicated. After incubation for 30 min at room temperature, reactions were quenched with 0.5 µL 1 M Tris-HCl, pH 8, and run on 10% SDS-PAGE gels. The proteins were transferred to nitrocellulose and probed with an α-His primary antibody and HRP-conjugated goat α-mouse secondary antibody using standard methods.

RESULTS

Hrq1 and Pso2 repair a variety of ICLs

All ICLs are covalent linkages between complementary strands of DNA, but ICL-inducing agents vary in DNA sequence preference and how they affect DNA structure (reviewed in (34)). Indeed, ICL repair pathway utilization in mammals varies depending on the types of crosslinkers being used. For example, highly DNA-distorting lesions like cisplatin and nitrogen mustard ICLs are repaired via the canonical FA pathway (1), whereas psoralen- and abasic-induced ICLs are preferentially unhooked via the NEIL3 DNA glycosylase in a FA-independent manner (35). To determine if the Pso2-dependent ICL repair pathway in *S. cerevisiae* is dependent on the type of ICL formed, we tested the sensitivity of *pso2* mutants to several ICL-inducing agents. First, we examined the sensitivity of *pso2Δ* cells to mitomycin C (MMC), 8-methoxypsoralen (8-MOP) + UVA, and diepoxybutane (DEB). As diagrammed in Figure 1, MMC does not distort the DNA backbone, 8-MOP + UVA leads to ~25° unwinding of the DNA around the lesion, and DEB bends the DNA. Further, all three ICL inducing agents target different DNA sequences. Regardless of the type of ICL formed, deletion of *PSO2* severely sensitized cells to each type of ICL (Fig. 1). Similar to cells lacking *PSO2* and previously reported results (3,24), deletion of *HRQ1* also rendered cells sensitive to the various ICL-inducing

agents (Fig. 1), though Hrq1 does not appear to be as important in ICL repair as Pso2 because *hrq1Δ* cells were less sensitive to ICL damage than *pso2Δ* cells. Importantly, the deletion of both *HRQ1* and *PSO2* phenocopied the *pso2Δ* level of sensitivity, consistent with Hrq1 functioning in the Pso2-dependent pathway. The observed sensitivity of these mutants is specific to ICL damage as neither *pso2Δ* nor *hrq1Δ* cells were sensitive to the DNA alkylating agent methyl methanesulfonate (MMS) (36) (Fig. 1).

Hrq1 helicase activity is required for the repair of MMC ICLs (24), so we also tested the sensitivity of cells encoding *hrq1-K318A*, a helicase-dead mutant of Hrq1, to DEB and 8-MOP + UVA. We found that the *hrq1-K318A* mutant is more sensitive to ICLs compared to the *hrq1Δ* strain (Fig. 1). These results suggest that Hrq1-K318A is recruited to the lesion but is perhaps blocking Pso2 or other redundant repair pathways from accessing the site of damage. Because the *hrq1-K318A* strain is slightly less sensitive than *pso2Δ*, however, some amount of Pso2 or a compensatory pathway likely still has access to repair the lesion. This contrasts with the *pso2-H611A* nuclease-dead mutant, which phenocopies *pso2Δ*. These results suggest that Hrq1 may be directly recruited to DNA ICLs and that it may work with Pso2 to repair these lesions.

Hrq1 stimulates Pso2 nuclease activity

Our genetic analyses suggested that Hrq1 may have a direct role in ICL processing alongside Pso2. Indeed, there is a rich literature of RecQ family helicases and nucleases working in tandem (37,38). To investigate this further, we purified recombinant Pso2 and tested it for nuclease activity on blunt dsDNA. Similar to previous work with Pso2 (17), we observed 5′ phosphate-dependent 5′ → 3′ exonuclease activity (Fig. 2A). Here, only the radiolabelled oligonucleotide was phosphorylated to select for digestion of one strand (Supplemental Fig. 1A). In the presence of Hrq1, Pso2 nuclease activity increased in a concentration dependent manner up to a nearly threefold stimulation (Fig. 2B). At 200 nM, Pso2 digested ~80% of the full-length substrate, while 50 nM Pso2 was able to digest nearly as much DNA upon the addition of 150 nM Hrq1. To verify that our observed nuclease activity was due to Pso2 and not a contaminant from *E. coli*, we purified the nuclease-dead Pso2-H611A mutant and tested its nuclease activity. Importantly, Pso2-H611A showed no nuclease activity above background, and no stimulation of the mutant was observed in the presence of Hrq1 (Fig. 2C and Supplemental Fig. 1B). Because Hrq1 helicase activity was required for ICL repair *in vivo* (Fig. 1), we also assayed the catalytically inactive Hrq1-K318A for stimulation of Pso2 nuclease activity *in vitro*. Hrq1-K318A was unable to increase Pso2 nuclease activity, suggesting that Hrq1 catalytic activity is essential to stimulate Pso2 (Supplemental Fig. 1B). Taken together, the data indicate that Hrq1 stimulates the activity of Pso2.

Hrq1 promotes Pso2 digestion through an ICL

It has been reported that Pso2 lacks translesional nuclease activity *in vitro*, being unable to degrade DNA past a site-specific ICL (17). However, the human homolog of Pso2, SNM1A, does display *in vitro* translesion exonuclease activity (13). Because Hrq1 can stimulate Pso2 nuclease activity on

undamaged DNA, we hypothesized that Hrq1 may also stimulate its translesional nuclease activity across an ICL. Thus, we next performed nuclease assays with a dsDNA substrate containing an ICL 7-nt from the 5′ end of the phosphorylated (*i.e.*, the digested) strand. To make this substrate, we used an established protocol to form ICLs from abasic sites *in vitro* (30). These ICLs are site specific and produced at high yields (up to ~70% crosslinks), which is advantageous relative to the difficult-to-make drug-based ICLs (34). Semlow *et al.* show that the repair of ICLs from abasic sites proceeds via the same mechanism that repairs psoralen ICLs (35), suggesting that this type of lesion is functionally equivalent to ICLs induced by small molecules.

After incubating Pso2, Hrq1, or both with the ICL-containing substrate, we measured the fraction of DNA larger than ~25-nt (pre-ICL) and compared it to the amount of translesion nuclease product <20-nt (post-ICL) (Supplemental Fig. 2). Contrary to previous work suggesting that Pso2 is unable to digest through ICLs (17), we found that Pso2 alone has weak translesion nuclease activity (Supplemental Fig. 2). However, we observed a significant increase in the post-ICL product when Hrq1 was present ($p < 0.05$). There are several technical challenges associated with working with DNA substrates harbouring an ICL *in vitro*, with the most notable issue being separation of the duplex DNA on denaturing gels and the resolution of the nuclease products.

Although the data (Supplemental Fig. 2) suggest the possibility of translesion nuclease activity by Pso2 in the presence of Hrq1, the gel-based assays did not provide a definitive answer. To accomplish this, we utilized single-molecule Förster resonance energy transfer (smFRET) to measure Pso2 nuclease activity. To observe nuclease activity, we prepared a DNA substrate that contains Cy3, Cy5, and biotin in the undigested strand, which was annealed to an unlabelled but 5'-phosphorylated strand to be digested by Pso2 (Fig. 3A). Because the FRET efficiency reports on the distance between the donor and acceptor, the FRET signals of dsDNA and ssDNA can be distinguished as low and high FRET, respectively (31). Therefore, the changes in FRET signal as ssDNA is released by Pso2 digestion of the unlabelled strand can be used to measure nuclease activity. Thus, we expect to see no change in FRET in the initial phase of Pso2 loading, followed by FRET increase induced by Pso2 digestion and concomitant generation of ssDNA and subsequent high FRET state resulting from the completion of the digestion (Fig. 3A).

To calibrate the smFRET system, we measured FRET from the dsDNA substrate and unannealed ssDNA as undigested and completely digested controls, respectively. The FRET histograms of dsDNA and ssDNA produced sharp peaks at the expected values of 0.32 and 0.80, respectively (Fig. 3B). Next, we applied varying conditions of Pso2 and Hrq1 and collected images in 10-min intervals to measure the FRET change over time. Upon adding 50 nM Pso2 alone, < 10% of molecules shifted to high FRET after 30 min. However, longer time courses (> 40 min) of Pso2 nuclease activity revealed that Pso2 was able digest nearly 50% of the substrate (Supplemental Fig. 4A). When Hrq1 was added without Pso2, the FRET peak remained unchanged, consistent with the expectation that Hrq1 does not bind and unwind dsDNA (Supplemental Fig. 3) (3). In contrast, when 50 nM Pso2 and 150 nM Hrq1 were incubated together in our FRET assay, we observed a dramatic increase in high FRET signal within minutes. Approximately 76% of molecules were digested in 10 min, with nearly 100% of

the DNA digested by 30 min (Fig. 3C). These smFRET results are highly correlated to our gel-based assays (Fig. 2C), which also display significantly enhanced Pso2 nuclease activity by Hrq1 (Fig 2B).

Next, we compared the nuclease-helicase coupled activity on undamaged DNA vs. ICL-containing substrate (XL-DNA). In the absence of Hrq1, Pso2 digested 6% of the undamaged DNA in 10 min, but no activity was detected for Pso2 digestion of XL-DNA, indicating that Pso2 has little to no translesion nuclease activity alone. Even with longer incubation times and in contrast to undamaged DNA, Pso2 was unable to digest a measurable amount of XL-DNA (Supplemental Fig. 4B). Strikingly, in the presence of Hrq1, 62% of the XL-DNA substrate was digested by Pso2 (Fig. 4A and B). We then asked if the enhanced Pso2 activity requires ATP hydrolysis by Hrq1. To address this question, we conducted the FRET-based nuclease assay in the absence of ATP. Without ATP, Pso2 + Hrq1 digested only 17% of undamaged DNA and no XL-DNA after 10 min (Fig. 4B). These values are more comparable to Pso2 in the absence of Hrq1. Similarly, we measured Pso2 nuclease activity in the presence of the ATPase-dead Hrq1-K318A mutant, which yielded 8.5% digestion product for undamaged DNA and none for XL-DNA (data not shown), confirming that the ATPase activity of Hrq1 is essential for promoting Pso2 nuclease activity. Taken together, our ensemble biochemical analyses and single molecule data demonstrate that Hrq1 significantly stimulates Pso2 nuclease activity on both undamaged DNA and XL-DNA, and the enhancement requires the catalytic activity of Hrq1.

Eukaryotic RecQ4 sub-family helicases specifically stimulate Pso2

As stated above, it is not uncommon for helicases and nucleases to function together in DNA repair pathways, as observed with the extensive resection by Sgs1 and Dna2 in HR (39). To determine if the stimulation of Pso2 nuclease activity is a result of general helicase activity or specifically related to Hrq1, we tested RecQ4 sub-family helicases from different species for their ability to stimulate Pso2 nuclease activity. We also tested Sgs1, the other RecQ helicase in *S. cerevisiae* (homologous to BLM (40)), for its ability to stimulate Pso2 nuclease activity. Interestingly, both Hrq1 and RECQL4 were able to significantly stimulate Pso2 (Fig. 5). In contrast, the Hrq1 homolog in *Mycobacterium smegmatis*, called SftH (21), was unable to stimulate Pso2, suggesting this phenomenon is specific to eukaryotic RecQ4 helicases. It should be noted that the *M. smegmatis* genome does not encode a homolog of Pso2, so if SftH is involved in ICL repair, it likely functions via a different mechanism.

Sgs1 yielded a level of Pso2 stimulation that was intermediate between SftH and Hrq1/RECQL4, though it was not significant (p = 0.2). This suggests that the observed synergy with Pso2 is specific to eukaryotic RecQ4 sub-family helicases. However, while *sgs1Δ* cells are also sensitive to ICL damage, they are not epistatic to *hrq1Δ* (24), suggesting that Sgs1 does not function in the Pso2 ICL repair pathway. To investigate this, we performed epistasis analysis with all three of the *hrq1Δ*, *pso2Δ*, and *sgs1Δ* alleles. As shown in Figure 5C, we recapitulated the synergistic ICL sensitivity of the *hrq1Δ sgs1Δ* double mutant relative to either of the single mutants (24) and found that the same was true of the *pso2Δ sgs1Δ* double and *hrq1Δ pso2Δ sgs1Δ* triple mutants. Thus, *in vivo*, Sgs1 does not participate in the Pso2 ICL repair pathway, even in the absence of Hrq1.

While the results in Figure 5 suggest a direct interaction between Pso2 and eukaryotic RecQ4 sub-family helicases, it is also possible that Hrq1 and RECQL4 stimulate Pso2 nuclease activity indirectly by unwinding the DNA probe to provide a more accessible ssDNA substrate for Pso2. While all tested helicases were able to unwind a Y-shaped fork substrate (Supplemental Fig. 5), the blunt dsDNA substrate used in the nuclease assays was not unwound by Hrq1, RECQL4, or SftH *in vitro*, while Sgs1 was able to unwind blunt dsDNA. The inability of Hrq1 and RECQL4 to unwind a blunt DNA substrate is consistent with our previous work (3), while the ability of Sgs1 to unwind a similar substrate has been previously reported (41). Thus, the modest amount of Pso2 stimulation by Sgs1 shown in Figure 5 could be due to the helicase simply generating ssDNA for Pso2 to degrade, but Hrq1 and RECQL4 must function by a different mechanism. Taken together, these results suggest that Hrq1 and Pso2 directly interact to promote the digestion of ICL-containing lesions.

Hrq1 and Pso2 interact through their N-termini

To determine if Hrq1 and Pso2 directly interact, we performed protein-protein crosslinking using the primary amine targeting disuccinimidyl sulfoxide (DSSO). Incubation of 500 nM Hrq1 (the ~130 kDa band) with equimolar amounts of Pso2 in the presence of excess DSSO resulted in a high molecular weight species approximately 180 kDa in mass as revealed by a western blotting for the Hrq1 N-terminal His-tag (Fig. 6A). This product could correspond to an Hrq1-Pso2 crosslinked complex. Interestingly, the presence of this 180 kDa product was not dependent on the presence of DNA, but a molar excess of Hrq1 relative to Pso2 increased the amount of this species. This is consistent with our biochemical analyses that suggest a higher Hrq1:Pso2 ratio is optimal for nuclease stimulation (Fig. 2B).

We previously hypothesized that the disordered N-terminus of Hrq1 could be an important docking site for protein-protein interactions (3). Similarly, Pso2 is also predicted to possess an unstructured N-terminus (Supplemental Fig. 6A). To determine the role of the Pso2 N-terminus in Hrq1-mediated nuclease stimulation, we first compared the nuclease activity of full-length Pso2 to an N-terminal truncation of the first 94 residues (referred to as Pso2ΔN). Interestingly, we found that Pso2ΔN had significantly more nuclease activity than full-length Pso2 (Fig. 6B), suggesting that the Pso2 N-terminus is an autoinhibitory domain. This phenomenon is conserved in the human homolog of Pso2, SNM1A, whose N-terminal truncation is also more active *in vitro* (13). The addition of Hrq1 did not result in stimulation of Pso2ΔN (Fig. 6B), though the highly efficient nuclease activity of the truncation may have already been maximal when used at 20 nM, which is a concentration at which stimulation of full-length Pso2 by Hrq1 can be observed. To test this, we measured the nuclease activity of 2 nM Pso2ΔN, which has a more comparable amount of nuclease activity to 20 nM full-length Pso2 (Supplemental Fig. 6B). Hrq1 very mildly stimulated Pso2ΔN nuclease activity under these conditions, but not nearly to the levels of full-length Pso2. These data suggest the Pso2 N-terminus is an autoinhibitory domain that also interacts with Hrq1 to mediate the observed nuclease activity stimulation.

Because *M. smegmatis* SftH, was unable to stimulate Pso2, we hypothesized that its lack of a large, natively disordered N-terminal domain like Hrq1 and RECQL4 may be the reason for this difference. Thus, we measured stimulation of Pso2 by an Hrq1 N-terminal truncation of residues 1-279 (known as Hrq1ΔN). Hrq1ΔN was unable to stimulate Pso2 nuclease activity, suggesting the interaction interfaces for both proteins are their disordered N-termini (Fig. 6B). The *in vivo* activity of these mutants also supports this conclusion as the ICL sensitivity of cells expressing Hrq1ΔN rather than the full-length helicase phenocopied that of a strain completely lacking Hrq1, and *pso2⊿* and *pso2⊿N* cells were also similarly sensitive to ICL damage (Fig. 6C).

DISCUSSION

The above analyses of the genetic and biochemical interaction between Hrq1 and Pso2 suggest that the mechanistic role of Hrq1 in the Pso2 ICL repair pathway is to stimulate the translesional nuclease activity of Pso2, facilitating efficient repair of ICLs from multiple sources. Our ensemble and single-molecule biochemistry results indicate that Pso2 alone is weakly able to digest DNA past a site-specific ICL, but Hrq1 greatly stimulates this activity in an ATP-dependent manner. This phenomenon is specific to the eukaryotic RecQ4 helicases, likely due to an NTD-to-NTD physical interaction between the helicase and nuclease. Importantly, these results explain why *recql4* mutant cell lines are sensitive to ICLs, and this DNA damage repair deficiency may underlie the genomic instability characteristic of RECQL4-linked diseases.

Implications for FA-independent ICL repair across evolution

It is clear that the FA pathway is the key ICL repair pathway in metazoans during S-phase (1), but it has more recently been appreciated that FA-independent ICL repair occurs in other *in vivo* contexts, such as during other phases of the cell cycle and when RNA polymerase encounters an ICL (9,42). In non-metazoan organisms, the FA pathway is also not the dominant ICL repair pathway or absent altogether. For instance, *S. cerevisiae* predominantly uses the Pso2 repair pathway but contains a rudimentary FA pathway containing obvious homologs of some of the metazoan enzymes involved in ICL repair (2,14). However, FA homologs appear to be lacking in prokaryotes, and thus, additional solutions to ICL repair must exist.

The data presented here and in our previous work (26) indicate that the Hrq1 helicase is involved in FA-independent ICL repair. This mirrors what is known about human RECQL4 in ICL repair in that *recql4* mutant cells are sensitive to the ICL-inducing drug cisplatin (25), and RECQL4 does not belong to any of the known FA complementation groups (43,44). Work on the Hrq1 homologs in *Schizosaccharomyces pombe* (45) and *A. thaliana* (23) also supports a role for these helicases in ICL repair, and the more distantly related Hrq1 homolog in *Bacillus subtilis* named MrfA was recently reported to have a role in the repair of MMC-induced lesions (22), so the bacterial RecQ4 family helicases likely function in ICL repair and/or the repair of similar types of DNA damage. Although the function of archaeal RecQ4 helicases (also called SftH (21)) is, to our knowledge, completely

unexplored, it is tempting to speculate that they are also involved in ICL repair based on homology to their bacterial and eukaryotic homologs.

Regardless, the involvement of RecQ4 family helicases in ICL repair across 3 billion years of evolution may indicate that the repair pathway in which these helicases function is one of the original mechanisms that developed to combat ICL damage, with the FA pathway evolving much later. ICL repair is a critical genome stability pathway, not just in the face of bi-functional exogenous compounds that cause ICLs but also due to endogenous sources of ICL damage. For instance, acetaldehyde is a metabolite produced during ethanolic fermentation that can cause DNA ICLs. It accumulates intracellularly (46), especially when exogenous ethanol concentrations are low (47), and thus ICLs are more apt to occur during the early stage of fermentation. Although we did not test *hrq1Δ* or *pso2Δ* cells for sensitivity to endogenous sources of ICLs, sensitivity of *hrq1* mutants to acetaldehyde-derived ICLs would explain why *HRQ1*/*hrq1Δ* diploids display haploinsufficiency specifically during the early phase of wine fermentation but not later stages when the exogenous ethanol concentration is high (48).

In light of the evolutionary importance of Hrq1-type helicases and ICL repair, it should be noted that not all prokaryotes encode a RecQ4 helicase, with *E. coli* being a prime example. In such organisms, ICL repair is performed by the concerted activities of the UvrABC endonuclease and recombination machinery (49,50). Similarly, not all organisms encode a homolog of Pso2/SNM1A (*e.g.*, *B. subtilis* and *M. smegmatis*), so other nucleases that function with RecQ4 helicases in ICL repair in such species remain to be identified. It is also likely that other factors in these pathways await discovery. In the case of *S. cerevisiae* Hrq1 and Pso2, what recruits these enzymes to the site of the ICL, are they the only proteins responsible for degradation of one strand of the crosslinked DNA and unhooking of the ICL, and what dictates the choice of ICL repair pathway (Hrq1/Pso2 *vs.* the FA-like pathway)? It is our hope that continued work in the yeast model will answer these questions and begin to shed light on the roles of RECQL4, SNM1A, and other factors in human ICL repair.

How does Hrq1 stimulate Pso2?

Our genetic and biochemical analyses of the Pso2 N-terminus suggest that it is important for ICL repair and likely acts as the protein-protein interaction interface for Hrq1. Thus, it is possible that Hrq1 and Pso2 form a complex in which Hrq1 translocates 3′ → 5′ along the undigested strand, while Pso2 degrades the complementary strand in the 5′ → 3′ direction in a mechanism similar to the Sgs1-Dna2 helicase-nuclease complex used in DSB repair (38). Alternatively, Hrq1 and Pso2 may interact more dynamically and specifically when Pso2 stalls. We found that Pso2 alone had very low nuclease activity and processivity (Fig. 2A), which is sufficient for digestion of the short (20-40 nt) excision substrate produced by NER factors in ICL repair. When Pso2 stalls randomly on undamaged DNA or specifically at an ICL, Hrq1 may eject the unproductive nuclease to allow rebinding of Pso2 to continue DNA degradation. A similar model has been proposed for the Hrq1 stimulation of telomerase (51).

The requirement of Hrq1 catalytic activity to stimulate Pso2 suggests that Hrq1 does not promote nuclease activity simply by inducing a conformational change in Pso2. However, this could be a component of the mechanism, especially when considering the autoinhibitory nature of the Pso2 N-terminal domain. Hrq1 could interact with the Pso2 N-terminus such that it conformationally prohibits the Pso2 N-terminus from inhibiting nuclease activity. While our data indicate that this is not the sole explanation for Hrq1-mediated stimulation of Pso2 nuclease activity, we cannot exclude this proposed phenomenon as a possible component of the mechanism of stimulation. Regardless, specifically identifying how Hrq1 stimulates Pso2 nuclease activity will be important when translating this model to human RECQL4 and SNM1A.

Regulation of Pso2 nuclease activity

Why does Pso2 need to be stimulated by Hrq1 for appropriate ICL resistance? Pso2 expression is extremely low, and ICL damage results in only a mild ~4-fold induction of Pso2 ((52), unpublished observations). The overexpression of Pso2 in yeast is extremely toxic (Supplemental Fig. 7), and the Pso2 N-terminus autoinhibits nuclease activity, providing another regulatory mechanism to prevent rampant Pso2 digestion. Thus, Pso2 expression is in a delicate balance between being sufficient for ICL repair and nucleotoxic. Coupling Hrq1 to Pso2 in ICL repair allows for modulated, site-specific nuclease activity. In this scenario, Hrq1 and Pso2 are recruited to ICLs via a currently unknown mechanism, and low levels of Pso2 are sufficient for ICL degradation, as Hrq1 is present to stimulate translesion exonuclease activity (Fig. 7). This scheme allows for cells to maintain a low Pso2 concentration but still have the appropriate amount of nuclease activity at the lesion. In the absence of Hrq1, Pso2 is still recruited to ICLs and can aid in their repair, but the process is less efficient, accounting for the mild ICL sensitivity of *hrq1Δ* cells (Fig. 1). Finally, in the absence of Pso2 itself, other pathways can repair some amount of the lesions (*e.g.*, the *S. cerevisiae* proto-FA pathway (14)), but many ICLs likely persist, resulting in mutagenesis and cell death (Fig. 7).

These data provide evidence for a novel role in ICL repair for RecQ4 helicases and further support the model that translesion nuclease activity by Pso2 is an important step in ICL repair. Because components of this mechanism are likely conserved in all domains of life, future work will be required to identify new proteins that facilitate RecQ4-medicated ICL repair and determine how RecQ4 helicases operate across evolution. How cells utilize such a diverse set of tools for ICL repair is likely determined by the molecular context in which the lesions are encountered, and pathway choice is an important but largely unexplored element of ICL repair.

ACKNOWLEDGEMENTS

We thank Drs. Hengyao Niu and Petr Cejka for the gift of recombinant Sgs1, Dr. Murray Junop for providing the Pso2 expression plasmid, Ms. Jade Katinas for purifying SftH, and members of the Bochman lab for useful discussions and critically reading this manuscript.

FUNDING

This work was supported by funds from the College of Arts and Sciences, Indiana University (to MLB); the Indiana University Collaborative Research Grant fund of the Office of the Vice President for Research (to MLB and YT); The American Cancer Society (RSG-16-180-01-DMC to MLB); the National Institutes of Health (1R35GM133437 to MLB, GM115631 to SM, and GM111695 to YT); and the National Science Foundation (MCB-1157688 to YT). Funding for open access charge: National Institutes of Health 1R35GM133437.

REFERENCES

1. Raschle, M., Knipscheer, P., Enoiu, M., Angelov, T., Sun, J., Griffith, J.D., Ellenberger, T.E., Scharer, O.D. and Walter, J.C. (2008) Mechanism of replication-coupled DNA interstrand crosslink repair. *Cell*, **134**, 969-980.
2. McHugh, P.J., Ward, T.A. and Chovanec, M. (2012) A prototypical Fanconi anemia pathway in lower eukaryotes? *Cell Cycle*, **11**, 3739-3744.
3. Rogers, C.M., Wang, J.C., Noguchi, H., Imasaki, T., Takagi, Y. and Bochman, M.L. (2017) Yeast Hrq1 shares structural and functional homology with the disease-linked human RecQ4 helicase. *Nucleic Acids Res*, **45**, 5217-5230.
4. Deans, A.J. and West, S.C. (2011) DNA interstrand crosslink repair and cancer. *Nature reviews. Cancer*, **11**, 467-480.
5. Liu, S. and Wang, Y. (2013) A quantitative mass spectrometry-based approach for assessing the repair of 8-methoxypsoralen-induced DNA interstrand cross-links and monoadducts in mammalian cells. *Anal Chem*, **85**, 6732-6739.
6. Datta, A. and Brosh, R.M., Jr. (2019) Holding All the Cards-How Fanconi Anemia Proteins Deal with Replication Stress and Preserve Genomic Stability. *Genes (Basel)*, **10**.
7. Zhang, J. and Walter, J.C. (2014) Mechanism and regulation of incisions during DNA interstrand cross-link repair. *DNA repair*, **19**, 135-142.
8. Huang, J., Liu, S., Bellani, M.A., Thazhathveetil, A.K., Ling, C., de Winter, J.P., Wang, Y., Wang, W. and Seidman, M.M. (2013) The DNA translocase FANCM/MHF promotes replication traverse of DNA interstrand crosslinks. *Mol Cell*, **52**, 434-446.
9. Andrews, A.M., McCartney, H.J., Errington, T.M., D'Andrea, A.D. and Macara, I.G. (2018) A senataxin-associated exonuclease SAN1 is required for resistance to DNA interstrand cross-links. *Nature communications*, **9**, 2592.
10. Kothandapani, A. and Patrick, S.M. (2013) Evidence for base excision repair processing of DNA interstrand crosslinks. *Mutat Res*, **743-744**, 44-52.
11. Kothandapani, A., Sawant, A., Dangeti, V.S., Sobol, R.W. and Patrick, S.M. (2013) Epistatic role of base excision repair and mismatch repair pathways in mediating cisplatin cytotoxicity. *Nucleic Acids Res*, **41**, 7332-7343.
12. Cattell, E., Sengerova, B. and McHugh, P.J. (2010) The SNM1/Pso2 family of ICL repair nucleases: from yeast to man. *Environ Mol Mutagen*, **51**, 635-645.
13. Wang, A.T., Sengerova, B., Cattell, E., Inagawa, T., Hartley, J.M., Kiakos, K., Burgess-Brown, N.A., Swift, L.P., Enzlin, J.H., Schofield, C.J. *et al.* (2011) Human SNM1A and XPF-ERCC1 collaborate to initiate DNA interstrand cross-link repair. *Genes Dev*, **25**, 1859-1870.
14. Ward, T.A., Dudasova, Z., Sarkar, S., Bhide, M.R., Vlasakova, D., Chovanec, M. and McHugh, P.J. (2012) Components of a Fanconi-like pathway control Pso2-independent DNA interstrand crosslink repair in yeast. *PLoS Genet*, **8**, e1002884.
15. Hazrati, A., Ramis-Castelltort, M., Sarkar, S., Barber, L.J., Schofield, C.J., Hartley, J.A. and McHugh, P.J. (2008) Human SNM1A suppresses the DNA repair defects of yeast pso2 mutants. *DNA repair*, **7**, 230-238.
16. Li, X., Hejna, J. and Moses, R.E. (2005) The yeast Snm1 protein is a DNA 5'-exonuclease. *DNA repair*, **4**, 163-170.
17. Tiefenbach, T. and Junop, M. (2012) Pso2 (SNM1) is a DNA structure-specific endonuclease. *Nucleic Acids Res*, **40**, 2131-2139.

18. Bernstein, K.A., Gangloff, S. and Rothstein, R. (2010) The RecQ DNA helicases in DNA repair. *Annual review of genetics*, **44**, 393-417.
19. Rogers, C.M., vanKessel, K.E. and Bochman, M.L. (Feb 2014) Helicases involved in the repair of DNA inter-strand crosslinks. *OA Biology*.
20. Barea, F., Tessaro, S. and Bonatto, D. (2008) In silico analyses of a new group of fungal and plant RecQ4-homologous proteins. *Comput Biol Chem*, **32**, 349-358.
21. Yakovleva, L. and Shuman, S. (2012) Mycobacterium smegmatis SftH exemplifies a distinctive clade of superfamily II DNA-dependent ATPases with 3' to 5' translocase and helicase activities. *Nucleic Acids Res*, **40**, 7465-7475.
22. Burby, P.E. and Simmons, L.A. (2019) A bacterial DNA repair pathway specific to a natural antibiotic. *Mol Microbiol*, **111**, 338-353.
23. Rohrig, S., Dorn, A., Enderle, J., Schindele, A., Herrmann, N.J., Knoll, A. and Puchta, H. (2018) The RecQ-like helicase HRQ1 is involved in DNA crosslink repair in Arabidopsis in a common pathway with the Fanconi anemia-associated nuclease FAN1 and the postreplicative repair ATPase RAD5A. *New Phytol*, **218**, 1478-1490.
24. Bochman, M.L., Paeschke, K., Chan, A. and Zakian, V.A. (2014) Hrq1, a Homolog of the Human RecQ4 Helicase, Acts Catalytically and Structurally to Promote Genome Integrity. *Cell reports*, **6**, 346-356.
25. Jin, W., Liu, H., Zhang, Y., Otta, S.K., Plon, S.E. and Wang, L.L. (2008) Sensitivity of RECQL4-deficient fibroblasts from Rothmund-Thomson syndrome patients to genotoxic agents. *Hum Genet*, **123**, 643-653.
26. Rogers, C.M. and Bochman, M.L. (2017) Saccharomyces cerevisiae Hrq1 helicase activity is affected by the sequence but not the length of single-stranded DNA. *Biochem Biophys Res Commun*, **486**, 1116-1121.
27. Sikorski, R.S. and Hieter, P. (1989) A system of shuttle vectors and yeast host strains designed for efficient manipulation of DNA in Saccharomyces cerevisiae. *Genetics*, **122**, 19-27.
28. Studier, F.W. (2005) Protein production by auto-induction in high density shaking cultures. *Protein Expr Purif*, **41**, 207-234.
29. Kanter, D.M. and Kaplan, D.L. (2011) Sld2 binds to origin single-stranded DNA and stimulates DNA annealing. *Nucleic Acids Res*, **39**, 2580-2592.
30. Price, N.E., Johnson, K.M., Wang, J., Fekry, M.I., Wang, Y. and Gates, K.S. (2014) Interstrand DNA-DNA cross-link formation between adenine residues and abasic sites in duplex DNA. *J Am Chem Soc*, **136**, 3483-3490.
31. Roy, R., Hohng, S. and Ha, T. (2008) A practical guide to single-molecule FRET. *Nature methods*, **5**, 507-516.
32. Lee, C.Y., McNerney, C. and Myong, S. (2019) G-Quadruplex and Protein Binding by Single-Molecule FRET Microscopy. *Methods Mol Biol*, **2035**, 309-322.
33. Lee, H.T., Bose, A., Lee, C.Y., Opresko, P.L. and Myong, S. (2017) Molecular mechanisms by which oxidative DNA damage promotes telomerase activity. *Nucleic Acids Res*, **45**, 11752-11765.
34. Guainazzi, A. and Scharer, O.D. (2010) Using synthetic DNA interstrand crosslinks to elucidate repair pathways and identify new therapeutic targets for cancer chemotherapy. *Cell Mol Life Sci*, **67**, 3683-3697.
35. Semlow, D.R., Zhang, J., Budzowska, M., Drohat, A.C. and Walter, J.C. (2016) Replication-Dependent Unhooking of DNA Interstrand Cross-Links by the NEIL3 Glycosylase. *Cell*, **167**, 498-511 e414.
36. Beranek, D.T. (1990) Distribution of methyl and ethyl adducts following alkylation with monofunctional alkylating agents. *Mutat Res*, **231**, 11-30.
37. Morimatsu, K. and Kowalczykowski, S.C. (2014) RecQ helicase and RecJ nuclease provide complementary functions to resect DNA for homologous recombination. *Proc Natl Acad Sci U S A*, **111**, E5133-5142.
38. Niu, H., Chung, W.H., Zhu, Z., Kwon, Y., Zhao, W., Chi, P., Prakash, R., Seong, C., Liu, D., Lu, L. *et al.* (2010) Mechanism of the ATP-dependent DNA end-resection machinery from Saccharomyces cerevisiae. *Nature*, **467**, 108-111.
39. Daley, J.M., Kwon, Y., Niu, H. and Sung, P. (2013) Investigations of homologous recombination pathways and their regulation. *Yale J Biol Med*, **86**, 453-461.
40. Cejka, P., Cannavo, E., Polaczek, P., Masuda-Sasa, T., Pokharel, S., Campbell, J.L. and Kowalczykowski, S.C. (2010) DNA end resection by Dna2-Sgs1-RPA and its stimulation by Top3-Rmi1 and Mre11-Rad50-Xrs2. *Nature*, **467**, 112-116.

41. Cejka, P. and Kowalczykowski, S.C. (2010) The full-length Saccharomyces cerevisiae Sgs1 protein is a vigorous DNA helicase that preferentially unwinds holliday junctions. *J Biol Chem*, **285**, 8290-8301.
42. Enoiu, M., Jiricny, J. and Scharer, O.D. (2012) Repair of cisplatin-induced DNA interstrand crosslinks by a replication-independent pathway involving transcription-coupled repair and translesion synthesis. *Nucleic Acids Res*, **40**, 8953-8964.
43. Duxin, J.P. and Walter, J.C. (2015) What is the DNA repair defect underlying Fanconi anemia? *Curr Opin Cell Biol*, **37**, 49-60.
44. Longerich, S., Li, J., Xiong, Y., Sung, P. and Kupfer, G.M. (2014) Stress and DNA repair biology of the Fanconi anemia pathway. *Blood*, **124**, 2812-2819.
45. Groocock, L.M., Prudden, J., Perry, J.J. and Boddy, M.N. (2012) The RecQ4 orthologue Hrq1 is critical for DNA interstrand cross-link repair and genome stability in fission yeast. *Mol Cell Biol*, **32**, 276-287.
46. Stanley, G.A. and Pamment, N.B. (1993) Transport and intracellular accumulation of acetaldehyde in saccharomyces cerevisiae. *Biotechnol Bioeng*, **42**, 24-29.
47. Stanley, G.A., Douglas, N.G., Every, E.J., Tzanatos, T. and Pamment, N.B. (1993) Inhibition and stimulation of yeast growth by acetaldehyde. *Biotechnology Letters*, **15, 1199-1204**.
48. Novo, M., Mangado, A., Quiros, M., Morales, P., Salvado, Z. and Gonzalez, R. (2013) Genome-wide study of the adaptation of Saccharomyces cerevisiae to the early stages of wine fermentation. *PLoS One*, **8**, e74086.
49. Cole, R.S. (1973) Repair of DNA containing interstrand crosslinks in Escherichia coli: sequential excision and recombination. *Proc Natl Acad Sci U S A*, **70**, 1064-1068.
50. Van Houten, B. and Snowden, A. (1993) Mechanism of action of the Escherichia coli UvrABC nuclease: clues to the damage recognition problem. *Bioessays*, **15**, 51-59.
51. Nickens, D.G., Rogers, C.M. and Bochman, M.L. (2018) The Saccharomyces cerevisiae Hrq1 and Pif1 DNA helicases synergistically modulate telomerase activity in vitro. *J Biol Chem*, **293**, 14481-14496.
52. Wolter, R., Siede, W. and Brendel, M. (1996) Regulation of SNM1, an inducible Saccharomyces cerevisiae gene required for repair of DNA cross-links. *Mol Gen Genet*, **250**, 162-168.

TABLE AND FIGURES LEGENDS

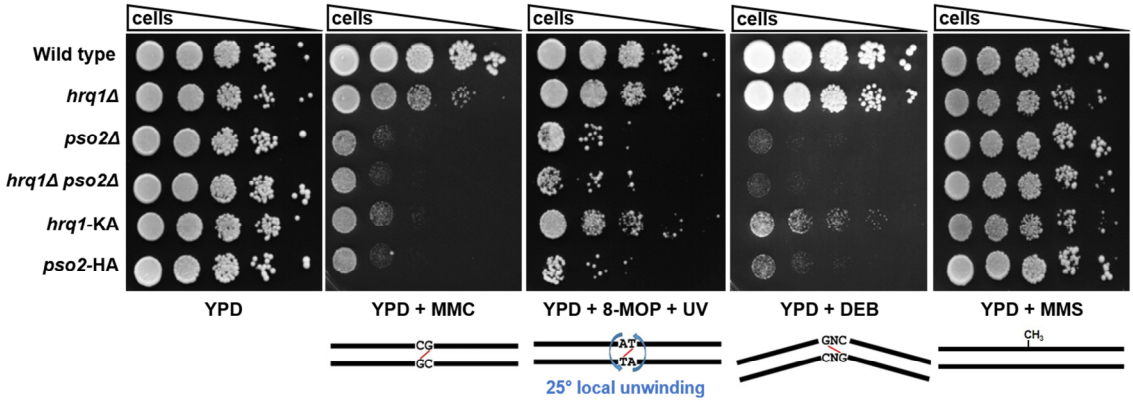

Figure 1. Hrq1 and Pso2 participate in the repair of many types of ICLs. Saturated overnight cultures of strains with the genotypes indicated on the left were diluted to OD_{660} = 1.0 and then further serially diluted 10-fold to 10^{-4}. Equal volumes of each dilution were then spotted onto rich medium (YPD) or rich medium supplemented with MMC, 8-MOP, DEB, or MMS. The plates containing 8-MOP were also exposed to UVA to activate the 8-MOP for crosslinking. The effect of the DNA damaging agent is diagrammed below each plate: MMC does not deform the DNA backbone, 8-MOP + UVA results in ~25° of local unwinding of the DNA around the lesion, DEB kinks the DNA backbone, and MMS alkylates the DNA.

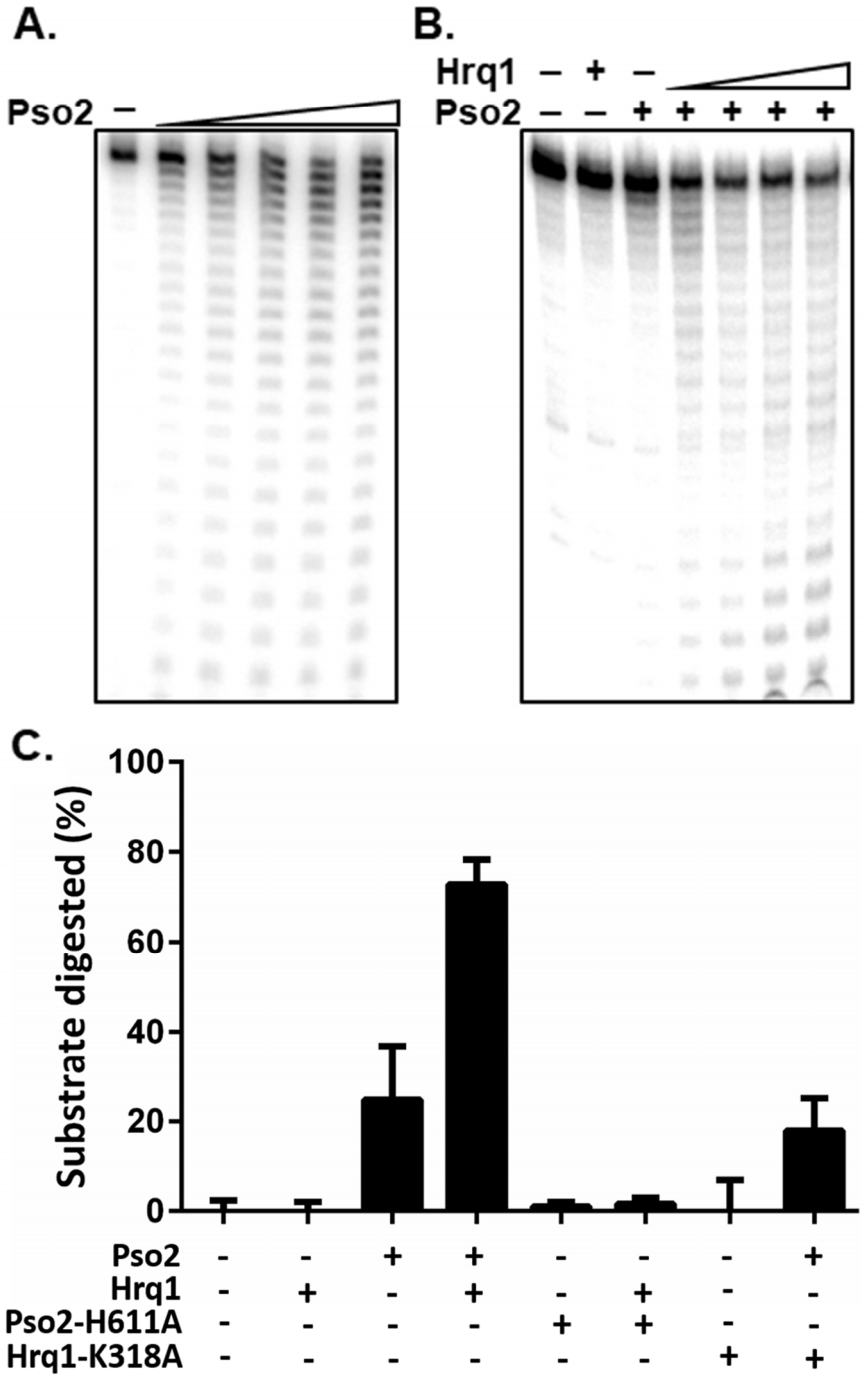

Figure 2. Hrq1 stimulates Pso2 nuclease activity. A) Concentration-dependent nuclease activity. Recombinant Pso2 (20-200 nM) was incubated with dsDNA for 30 min, and the nuclease products were separated on a denaturing gel. B) Hrq1-dependent stimulation of Pso2 nuclease activity. Denaturing gel showing the radiolabelled dsDNA substrate incubated alone, with 50 nM Pso2, 150 nM Hrq1, or 50 nM Pso2 and 20-150 nM Hrq1. C) Hrq1 requires catalytic activity to stimulate Pso2 nuclease activity. Quantification of the nuclease activity of Pso2 alone and in the presence of Hrq1 or the inactive Hrq1-K318A mutant. Nuclease-dead Pso2-H611A was used as a control. The graphed data are the averages of ≥ 3 independent experiments, and the error bars are the standard deviation (S.D.).

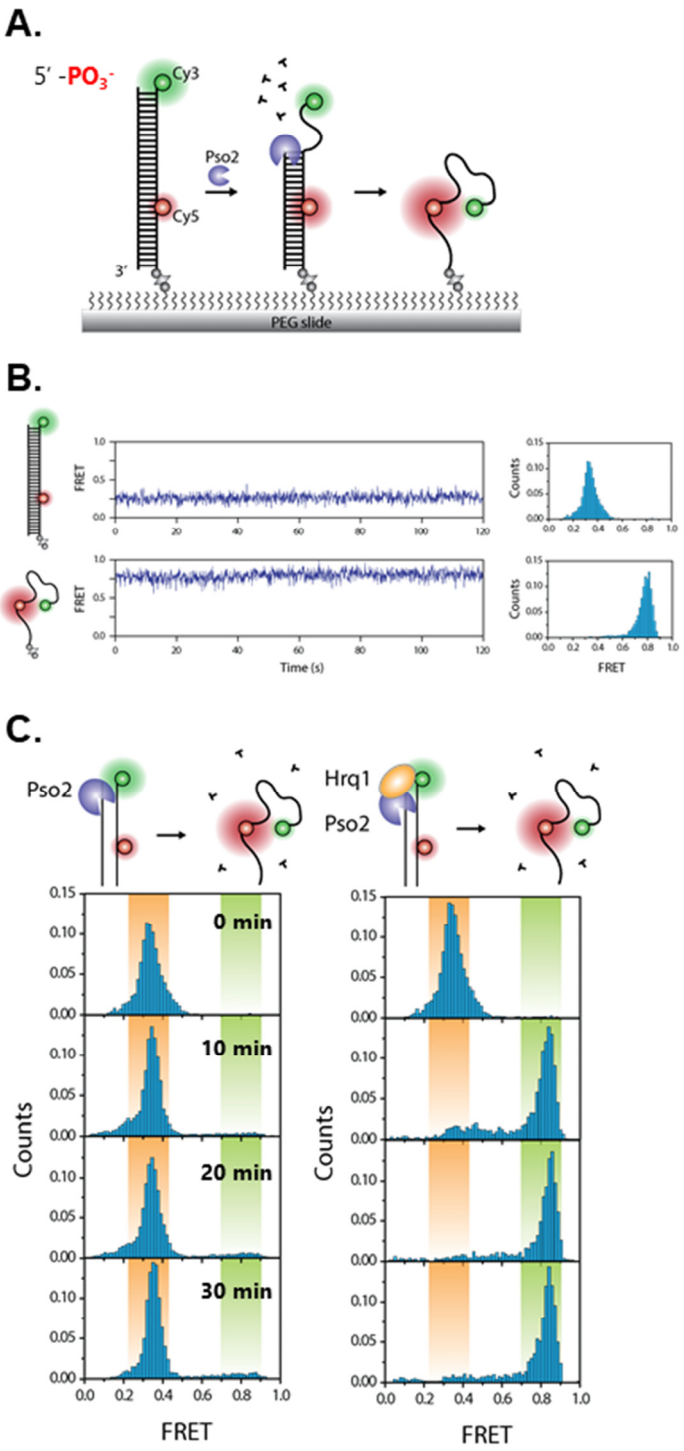

Figure 3. smFRET analysis of the stimulation of Pso2 nuclease activity by Hrq1. A) Diagram of the smFRET substrate and the effect of Pso2. Short lengths of dsDNA are rigid, keeping the Cy3 and Cy5 FRET pair distal from one another. Pso2 can digest away the unlabelled DNA strand, yielded flexible ssDNA and allowing the FRET pair to come into proximity. B) smFRET signal of the dsDNA substrate and the labelled ssDNA. C) Hrq1 stimulates Pso2 nuclease activity. Pso2 alone slowly generates an increase in the FRET signal by degrading the dsDNA substrate, but the addition of Hrq1 greatly increases the speed at which the high FRET signal appears.

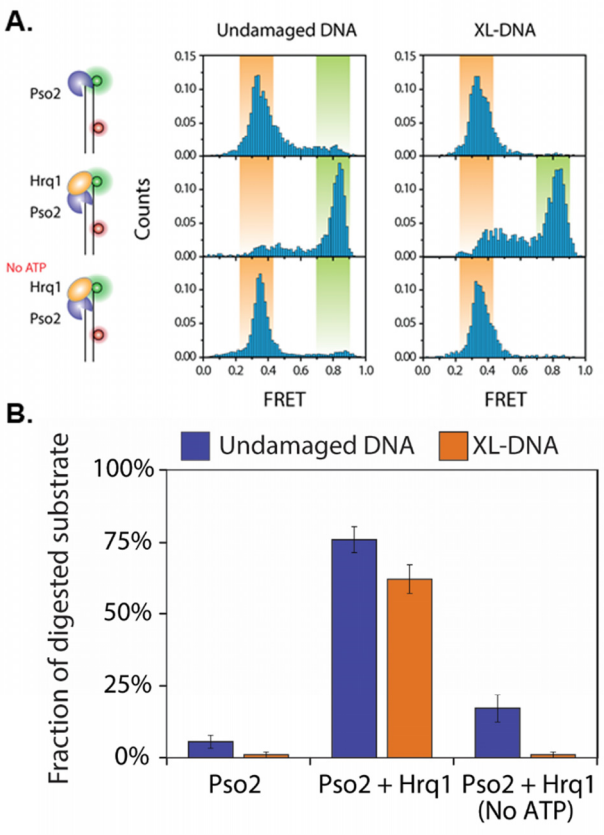

Figure 4. Hrq1 stimulates the translesion nuclease activity of Pso2. A) Pso2 lacks translesion nuclease activity in the absence of Hrq1. smFRET analysis of Pso2 activity on undamaged DNA and DNA with a site-specific ICL (XL-DNA) in the absence and presence of Hrq1. ATP is required to observe Pso2 stimulation by Hrq1. B) Quantification of the results from A. The error bars correspond to the S.D.

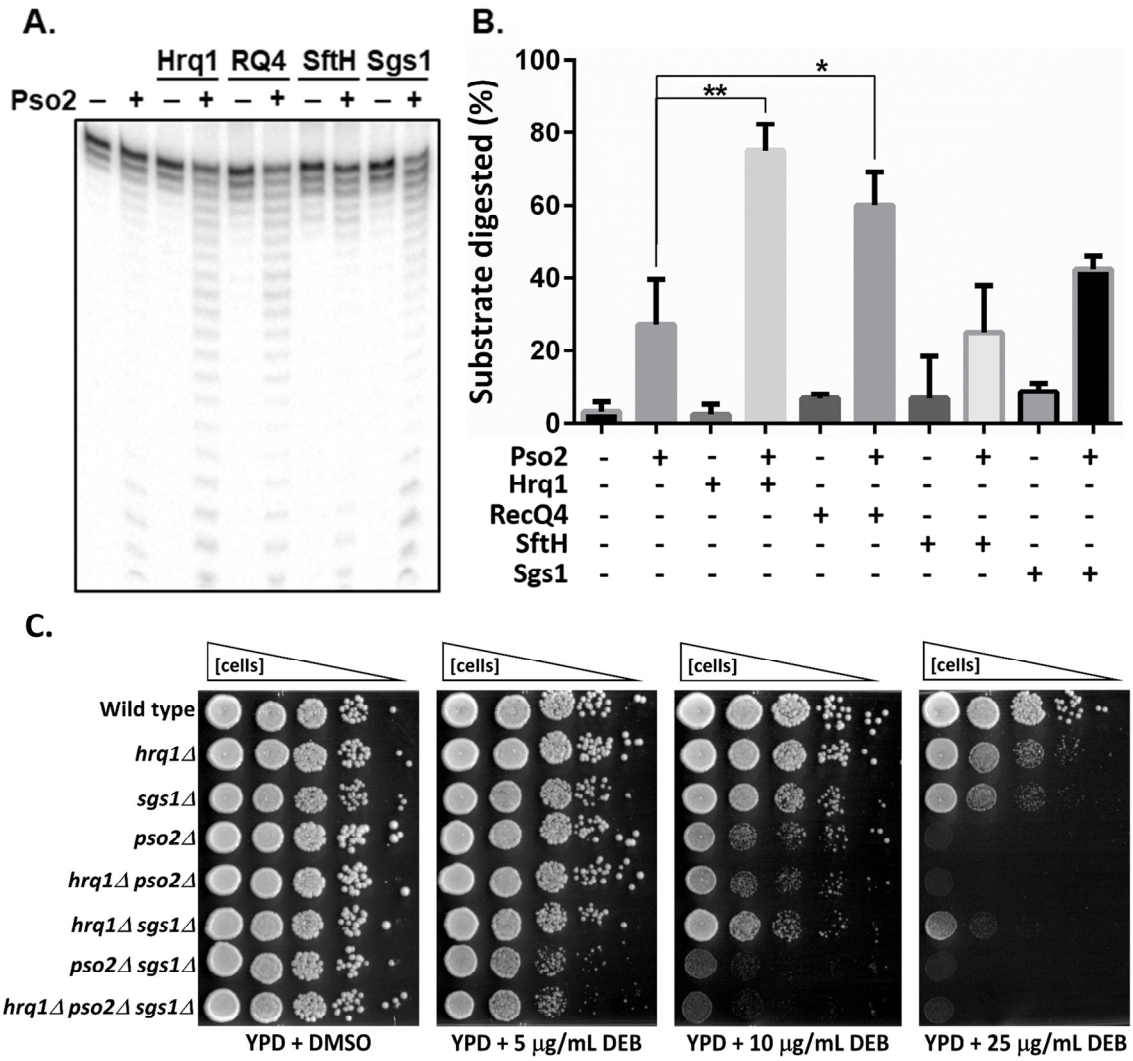

Figure 5. Eukaryotic RecQ4 subfamily helicases specifically stimulate Pso2 nuclease activity. A) Pso2 nuclease activity alone and in the presence of recombinant Hrq1, RECQL4, *M. smegmatis* SftH, or Sgs1. The radiolabelled dsDNA substrate was incubated with 50 nM Pso2 and/or 100 nM of the indicated helicase for 30 min, and nuclease products were separated on a denaturing gel and visualized by phosphorimaging. B) Quantification of ≥ 3 independent experiments performed as in A. The graphed data are the averages, and the error bars are the S.D. *, $p < 0.05$ and **, $p < 0.01$. Significant differences were determined by multiple *t*-tests using the Holm-Sidak method, with α = 5% and without assuming a consistent S.D. C) Deletion of *SGS1* is not epistatic to *hrq1Δ* or *pso2Δ*. Cells of the indicated genotypes were grown, diluted, and spotted onto YPD + DMSO or YPD + DEB plates as in Figure 1.

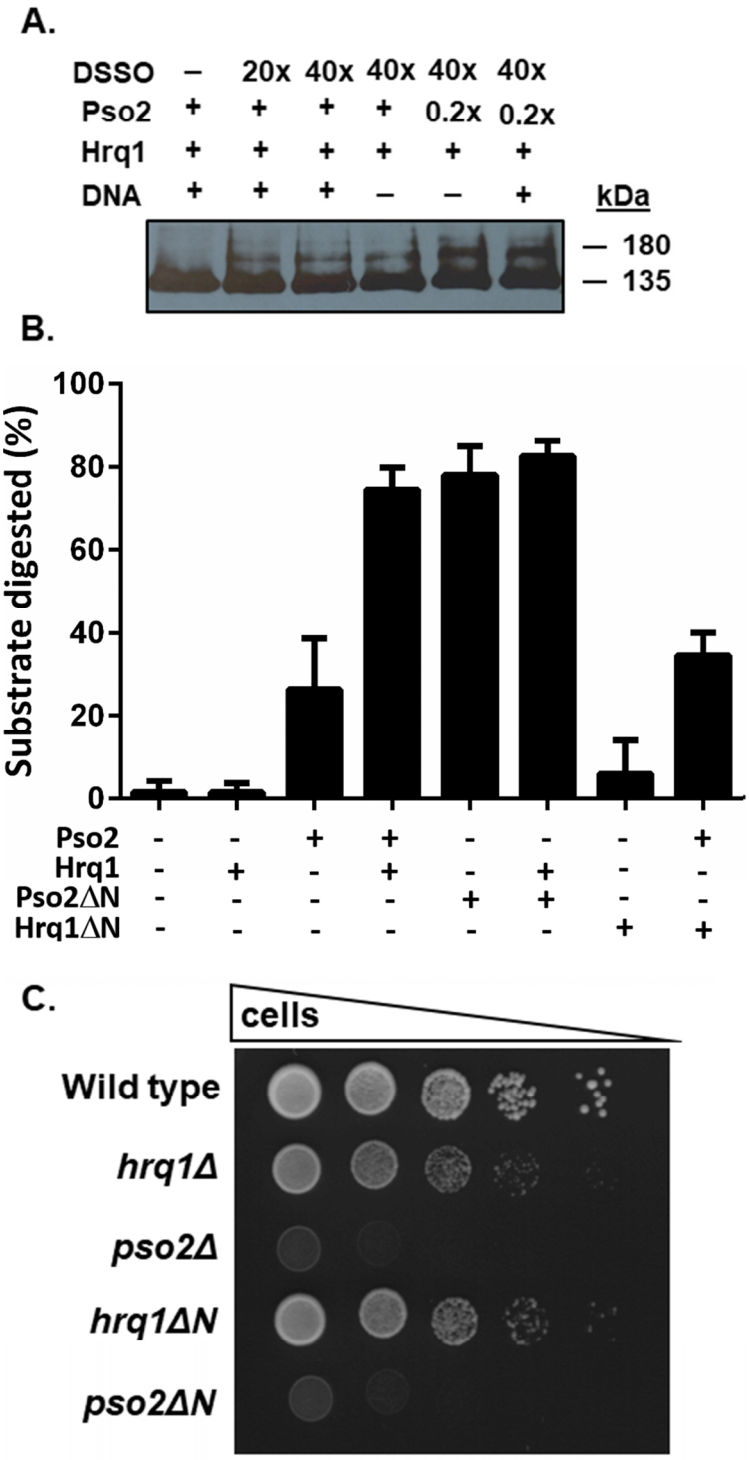

Figure 6. Hrq1 and Pso2 physically interact. A) Recombinant Hrq1 and Pso2 can be crosslinked in solution. Molar equivalents of Hrq1 and Pso2 were incubated in the presence or absence of 1 nM poly(dT) 50mer ssDNA and/or the presence or absence of a molar excess (20x or 40x) of the protein-protein crosslinker DSSO. The reactions were then analysed by SDS-PAGE and western blotting with an antibody recognizing the N-terminal 10xHis tag on Hrq1. Hrq1 alone produces a signal at the expected size of ~135 kDa, but the addition of Pso2 and DSSO yields a band of the approximate size of a Hrq1-Pso2 complex (~180 kDa). The amount of this slower migrating product increases when Hrq1 is present in a fivefold molar excess of Pso2 (0.2x), consistent with the optimal ratio of Hrq1:Pso2 in nuclease reactions. B) Nuclease activity of Pso2 and Pso2ΔN in the absence and presence of Hrq1 or Hrq1ΔN. The Hrq1ΔN truncation mutant fails to stimulate the nuclease activity of full-length Pso2, and Pso2ΔN alone has nuclease activity equivalent to Pso2+Hrq1. The graphed data are the means of ≥ 3 independent experiments, and the error bars are the S.D. C) The *hrq1ΔN* and *pso2ΔN* alleles phenocopy complete deletions of *HRQ1* and *PSO2*. Cells of the indicated genotypes were grown, diluted, and spotted onto YPD + DEB plates as in Figure 1.

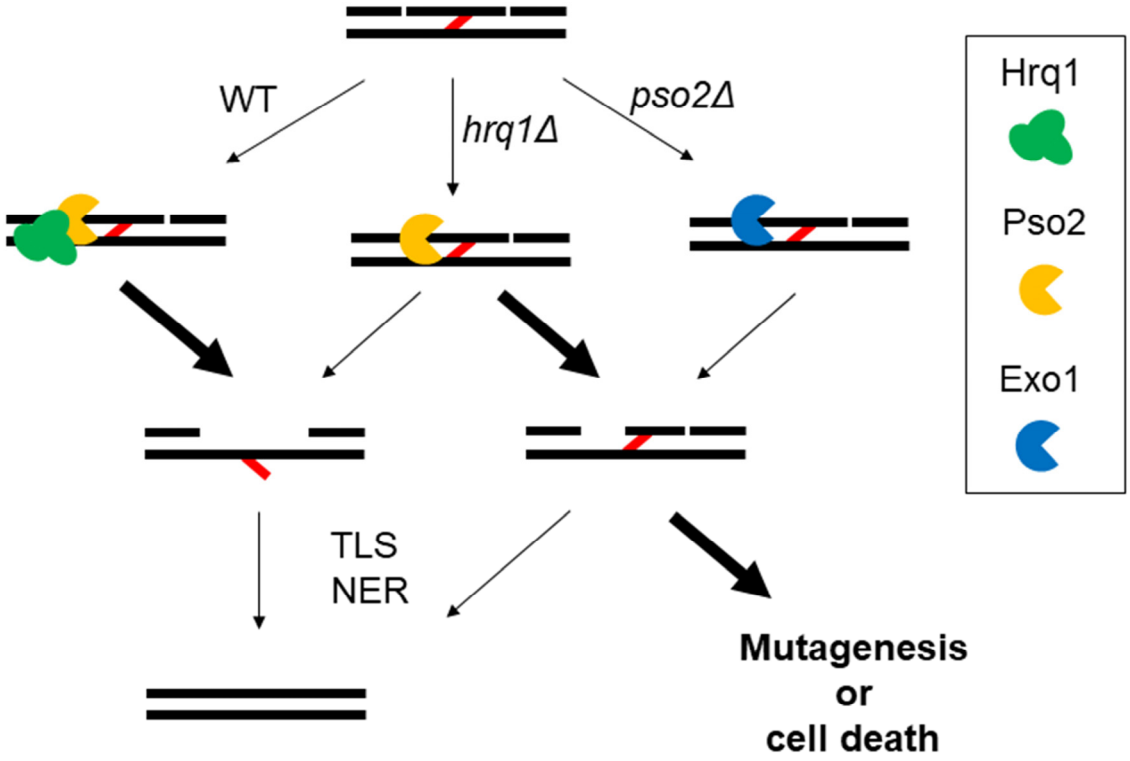

Figure 7. Model of ICL repair in WT, *hrq1Δ*, and *pso2Δ* cells. In the first step of ICL repair, the NER machinery cuts one strand of DNA on either side of the ICL. Then, in WT cells, Hrq1 and Pso2 are recruited to the lesion to digest away the incised strand, leaving an adducted base. TLS polymerases fill the gap, and NER removes the adducted base. In *hrq1Δ* cells, Pso2 is still recruited to the ICL, but its poor translesion nuclease activity in the absence of Hrq1 yields some amount of incompletely processed substrates, which can lead to mutagenesis or cell death. In cells lacking Pso2, other nucleases (*e.g.*, Exo1) may be recruited to ICLs, but there less optimal activity on such substrates can also lead to mutagenesis or cell death.

SUPPLEMENTAL MATERIALS AND METHODS

METHODS

Pso2 overexpression in *Saccharomyces cerevisiae*

Pso2 was cloned under the control of the galactose-inducible promoter in pESC-URA and transformed into cells deleted for *pso2*. Empty vector strains were also constructed. Overnight cultures were grown in uracil dropout medium supplemented with 2% raffinose. Cells were pelleted and washed with sterile H_2O before being added to a 96-well plate at an OD_{660} of 0.01 in uracil dropout medium supplemented with either 2% glucose or galactose. Cells were incubated at 30°C with vigorous shaking in a plate reader for 48 h, and OD_{660} readings were taken every 15 min. The resulting growth curves were used to calculate the mean OD_{660} for each condition. The mean values were taken from ≥ 3 independent experiments and averaged. The reported mean OD_{660} values were determined by dividing Pso2 overexpression strains by the mean OD_{660} of the empty vector strains in either glucose (repressed expression) or galactose (overexpression) as indicated.

Helicase assays

Helicase assays were performed as reported (3). Briefly, 2 nM labelled DNA substrate was incubated with the indicated helicase concentration in Nuclease Buffer with 5 mM ATP for 30 min at 30°C. For RECQL4 helicase assays, 15 nM cold ssDNA trap was added to capture the unwound product. The trap was added last along with ATP to start the reaction. Assays were stopped with 1x Stop-Load dye (5% glycerol, 20 mM EDTA, 0.05% SDS, and 0.25% bromophenol blue) and loaded onto 12% 19:1 acrylamide:bis-acrylamide nondenaturing gels and run in 1x TBE at 10 V/cm. Gels were dried under vacuum, imaged using a Typhoon FLA 9500, and quantified using ImageQuant 5.2.

SUPPLEMENTAL FIGURES

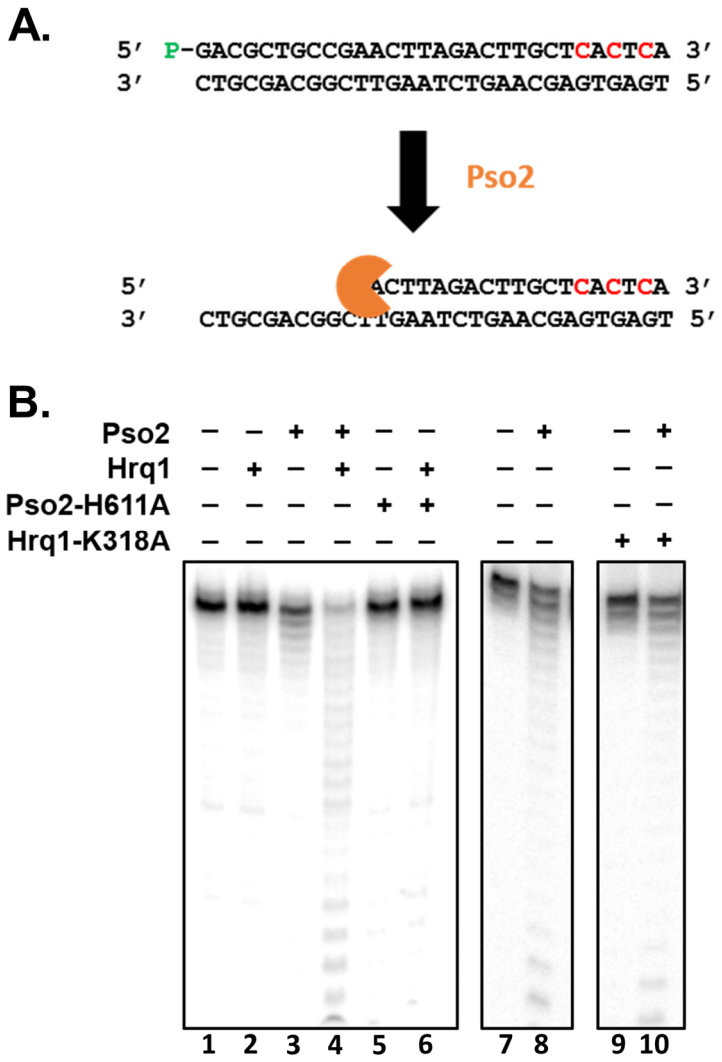

Supplemental Figure 1. Representative gel images of Hrq1-mediated Pso2 stimulation. A) Schematic of gel-based nuclease assay. The digested strand is 5′ phosphorylated and labelled on the 3′ end via Klenow fill-in (red nucleotides). Pso2 digestion is measured by the smaller bands as observed on denaturing gels. B) Nuclease activity of Pso2 or nuclease-dead Pso2-H611A in the presence or absence of Hrq1 or helicase-dead Hrq1-K318A. The indicated combination of enzymes (50 nM nuclease and 150 nM helicase) were incubated with dsDNA for 30 min. Lanes 1-6 were run on the same gel, whereas lanes 7-10 were identical conditions run on a separate gel (with intervening lanes removed for simplicity). Quantification of similar data from at least three independent experiments is reported in Figure 2C.

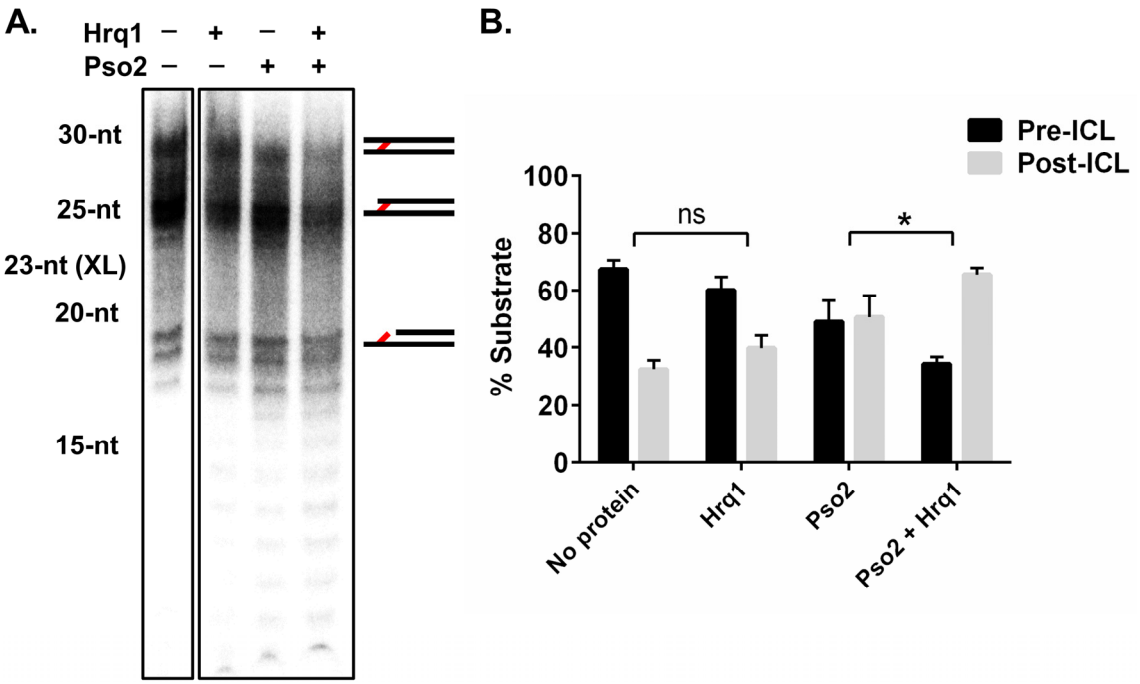

Supplemental Figure 2. Gel-based measurement of Pso2 nuclease activity on DNA containing a site-specific ICL (XL-DNA). A) Representative image of 200 nM Pso2 nuclease activity +/- 200 nM Hrq1 with dsDNA harbouring an ICL 7 nt from one blunt end. Size and representative schematic of products on the gel are presented on the left and right sides of the gel, respectively. B) Pso2 translesion nuclease activity is stimulated by Hrq1. Quantification of ≥ 3 independent experiments, and the error bars are S.D. Pre-ICL is defined by products digested prior to the ICL, whereas Post-ICL describes digestion products through the ICL. *, $p < 0.05$; not significant (n.s.), $p > 0.05$.

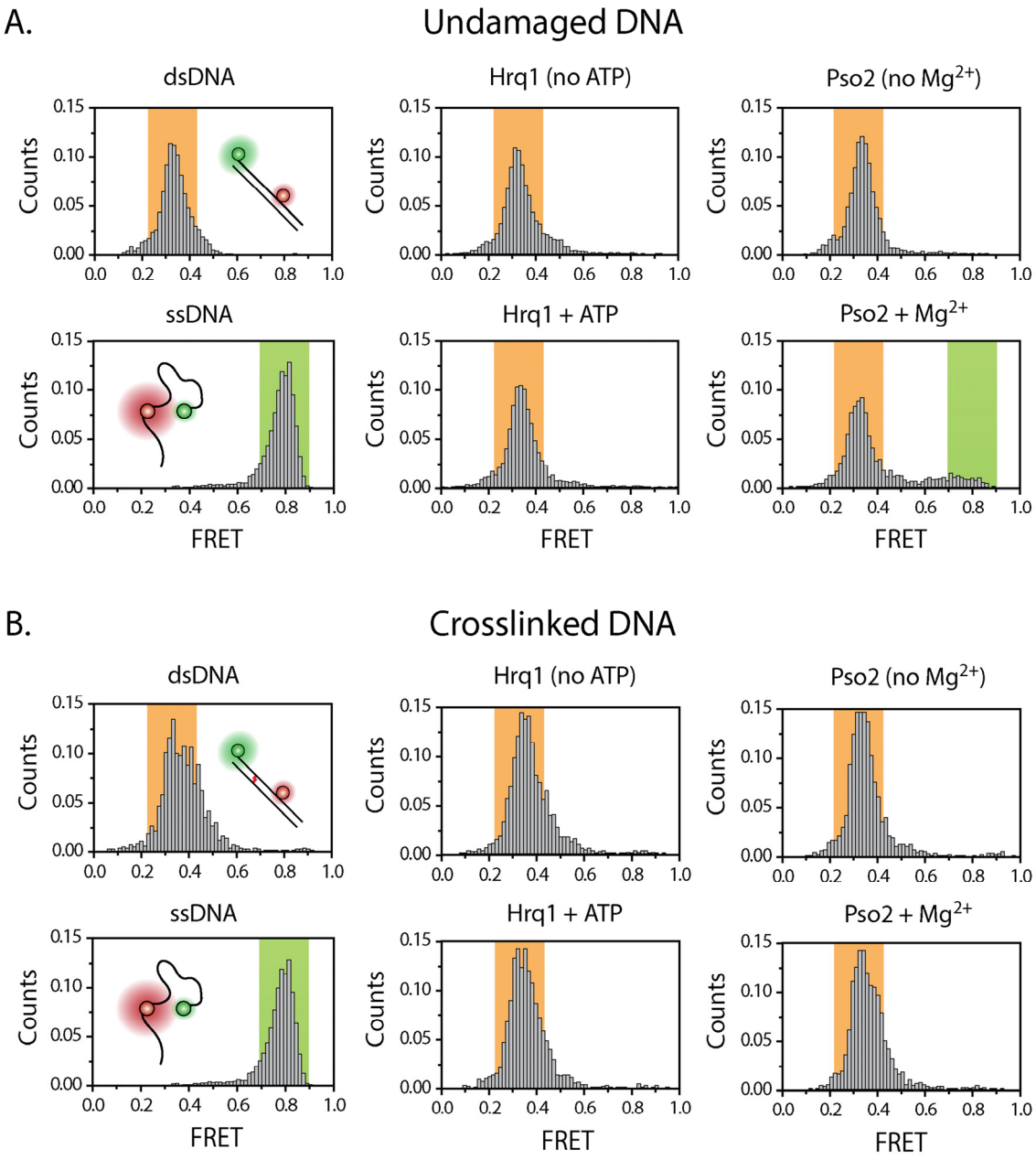

Supplemental Figure 3. Control smFRET nuclease assays. A) smFRET analysis on dsDNA under various conditions. The data used to plot the ssDNA and dsDNA histograms were collected in the absence of protein to determine the FRET values of digested and undigested substrate, respectively. Hrq1 +/- ATP had no effect on the substrate, as expected by previous experiments demonstrating a lack of Hrq1 helicase activity on similar blunt dsDNA substrates (3). Pso2 requires the presence of Mg^{2+} for nuclease activity. B) The same control experiments from A) were performed with XL-DNA.

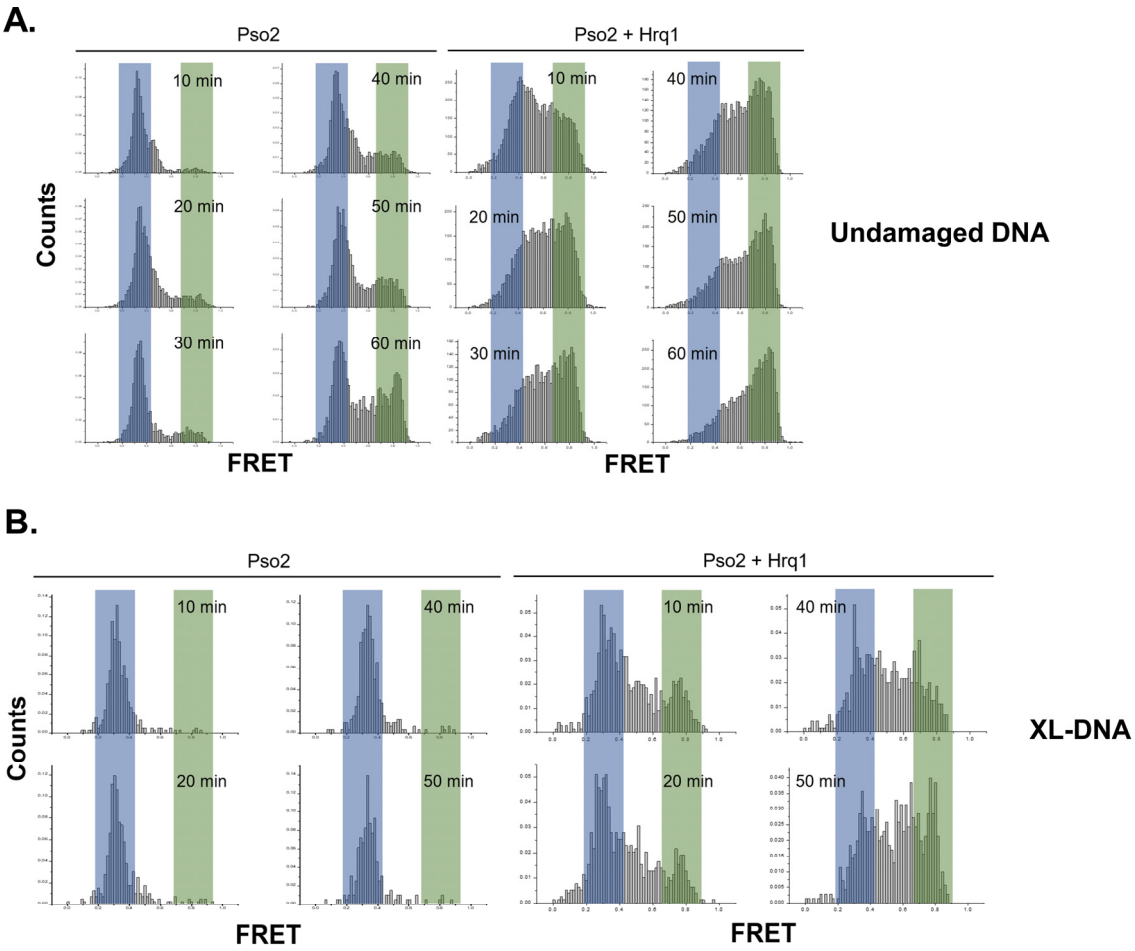

Supplemental Figure 4. A) smFRET analysis of Pso2 nuclease activity on undamaged dsDNA without and with Hrq1. B) smFRET analysis of Pso2 nuclease activity on XL-DNA without and with Hrq1.

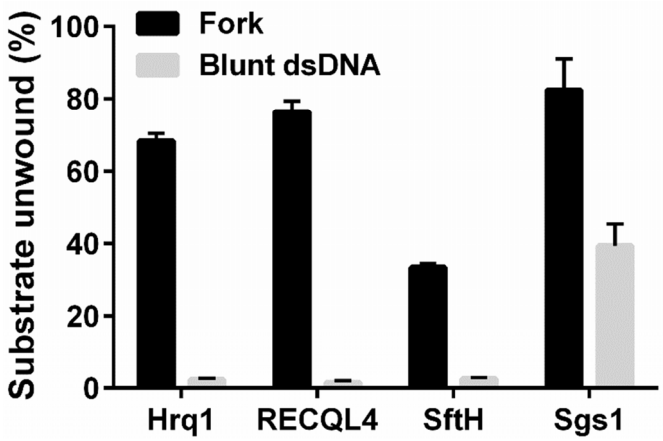

Supplemental Figure 5. Sgs1 unwinds the dsDNA substrate used in nuclease assays. Equimolar amounts of Hrq1, RECQL4, SftH, or Sgs1 were incubated for 30 min with either 2 nM Fork or dsDNA and quantified for helicase activity.

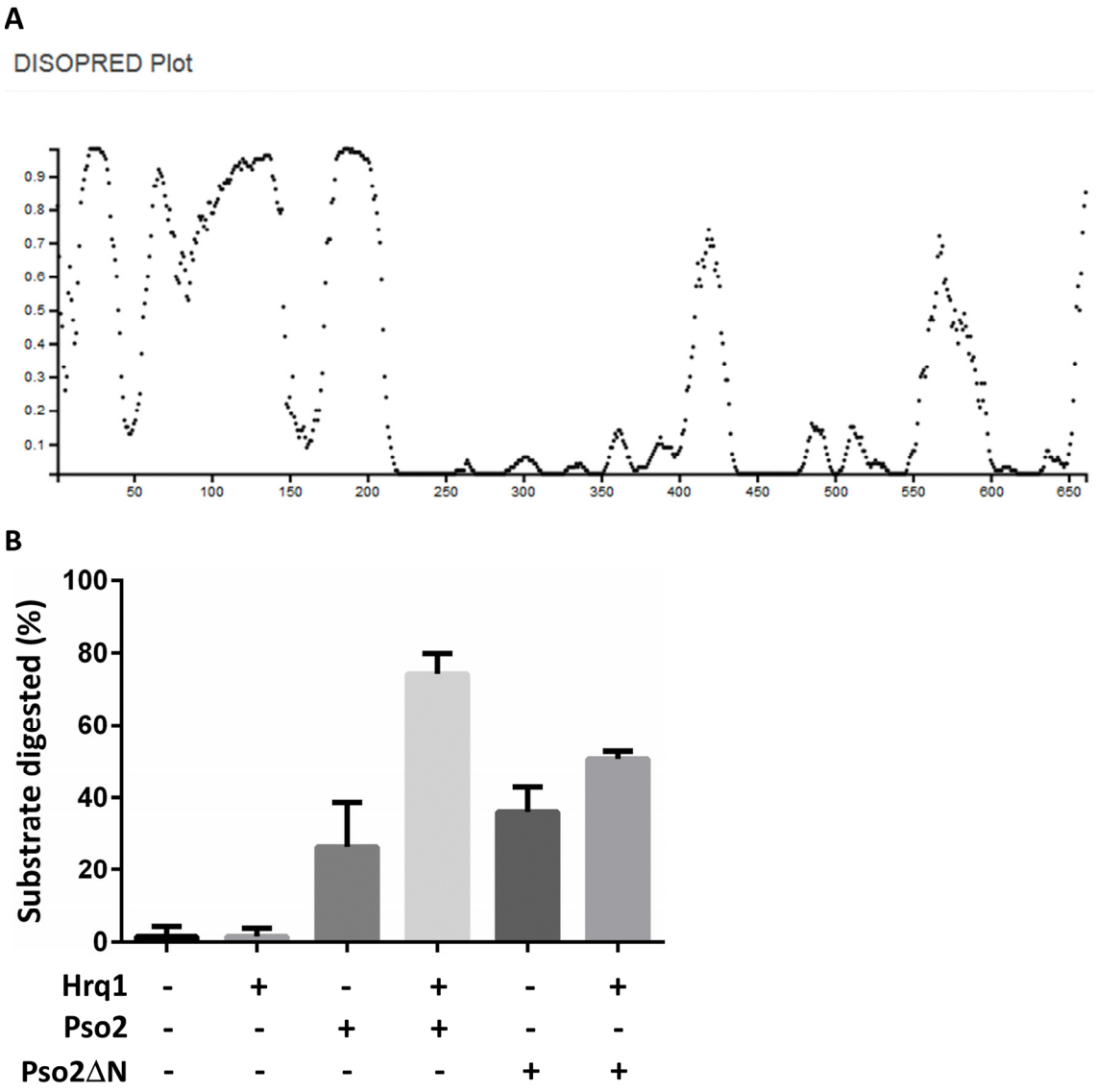

Supplemental Figure 6. The Pso2 N-terminus is an autoinhibitory domain. A) A DISOPRED profile for Pso2, as analysed by the UCL Department of Computer Science web server (http://bioinf.cs.ucl.ac.uk/psipred/?disopred=1) indicates that the N-terminal domain of Pso2 (aa 1~210) is predicted to be natively disordered. B) Hrq1 is unable to maximally stimulate Pso2ΔN. Pso2ΔN (50 nM) nearly completely digested the dsDNA substrate in Figure 4B, but here, 2 nM Pso2ΔN has comparable nuclease activity to 50 nM full-length Pso2. The addition of Hrq1 yielded very mild stimulation of Pso2ΔN nuclease activity at this concentration, suggesting that the N-terminus of Pso2 is required for Hrq1-mediated stimulation.

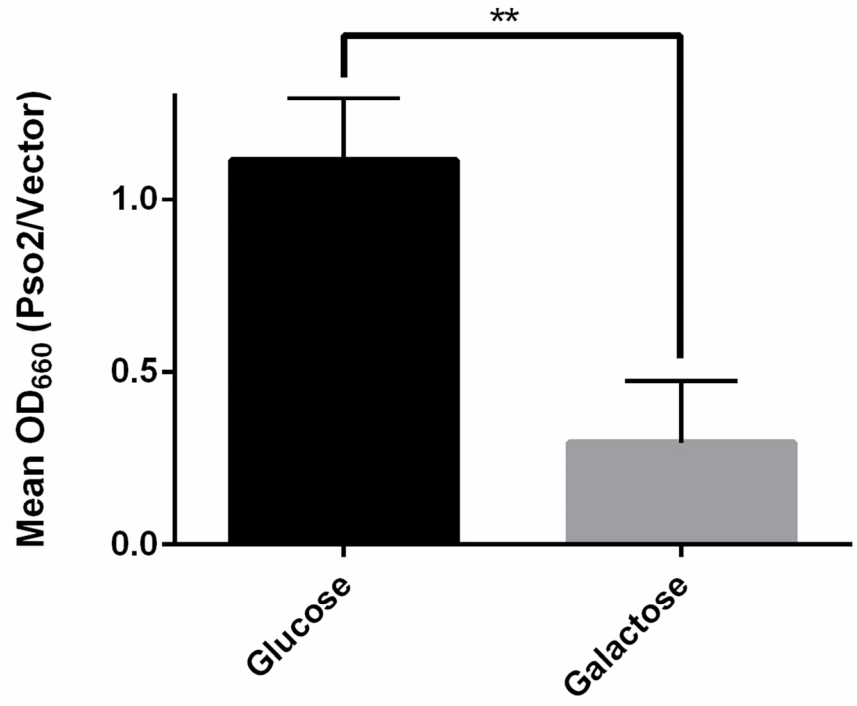

Supplemental Figure 7. Pso2 overexpression is toxic. Growth of cells harbouring a Pso2 overexpression vector in glucose, where Pso2 expression is repressed, is similar to that of the empty vector (Mean OD_{660} (Pso2/vector) of 1). Overexpression of Pso2 via galactose induction severely inhibits cell growth. ** $p < 0.001$.

Supplemental Table 1. Oligonucleotides used in this study.

Name	Sequence	Substrate
MB733	ACCGTTGTGCAACTGAGTGGACAACGTGTCACTCACATAGC GTTC	25-nt Random Fork, 5'-tail
MB734	GAACGCTATGTGAGTGACACCAACAGGTGAGTCAACGTGTT GCCA	25-nt Random Fork, 3'-tail
MB1614	/5Phos/GACGCTGCCGAACTTAGACTTGCT	Undamaged nuclease substrate
MB1461	TGAGTGAGCAAGTCTAAGTTCGGCAGCGTC	Undamaged nuclease substrate
MB1599	/5Phos/GACGAC/ideoxyU/TACTGCCGAGACTTGCT	ICL-containing substrate
MB1600	TGAGTGAGCAAGTCTCGGCAGTAAGTCGTC	ICL-containing substrate
MB1620	/5Phos/GACGAC/ideoxyU/TACTGCCGAGACATGCTCACTCA	ICL-containing smFRET substrate, digested strand
MB1621	/5Biosg/TGAGTGAGCA/iAmMC6T/GTCTCGGCAGTAAGTCGTC /3Cy3Sp/	smFRET substrate, labelled strand
MB1622	/5Phos/GACGACTTACTGCCGAGACATGCTCACTCA	Undamaged smFRET substrate, digested strand

Abbreviations: /5Phos/, 5' phosphate; /ideoxyU/, internal dU; ICL, inter-strand crosslink; smFRET, single-molecule Förster resonance energy transfer; /5Biosg/, 5' biotin; and /3Cy3Sp/, 3' Cy3 dye.

Supplemental Table 2. *Saccharomyces cerevisiae* strains used in this study.

Strain	Genotype	Origin
YHP499	*MATa ura3-52 lys2-801_amber ade2-101_ochre trp1Δ63 his3Δ200 leu2Δ1*	1
MBY321	*MATα ura3-52 lys2-801_amber ade2-101_ochre trp1Δ63 his3Δ200 leu2Δ1 hxt13::URA3 sgs1::his5+*	This work
MBY327	*MATα ura3-52 lys2-801_amber ade2-101_ochre trp1Δ63 his3Δ200 leu2Δ1 hxt13::URA3 sgs1::his5+ hrq1::TRP1*	This work
MBY462	*MATα ura3-52 lys2-801_amber ade2-101_ochre trp1Δ63 his3Δ200 leu2Δ1 hxt13::URA3 hrq1::His3MX6::Hrq1ΔN$^{1-279}$-NatMX*	This work
MBY686	*MATa ura3-52 lys2-801_amber ade2-101_ochre trp1Δ63 his3Δ200 leu2Δ1 pso2::pso2ΔN$^{1-94}$-His3MX6*	This work
MBY745	*MATa ura3-52 lys2-801_amber ade2-101_ochre trp1Δ63 his3Δ200 leu2Δ1 hrq1::His3MX6*	This work
MBY746	*MATa ura3-52 lys2-801_amber ade2-101_ochre trp1Δ63 his3Δ200 leu2Δ1 pso2::TRP1*	This work
MBY747	*MATa ura3-52 lys2-801_amber ade2-101_ochre trp1Δ63 his3Δ200 leu2Δ1 hrq1::His3MX6 pso2::TRP1*	This work
MBY748	*MATa ura3-52 lys2-801_amber ade2-101_ochre trp1Δ63 his3Δ200 leu2Δ1 hrq1::hrq1-K318A-His3MX6*	This work
MBY749	*MATa ura3-52 lys2-801_amber ade2-101_ochre trp1Δ63 his3Δ200 leu2Δ1 pso2::pso2-H611A-TRP1*	This work
MBY789	*MATa ura3-52 lys2-801_amber ade2-101_ochre trp1Δ63 his3Δ200 leu2Δ1 pESC-URA*	This work
MBY790	*MATa ura3-52 lys2-801_amber ade2-101_ochre trp1Δ63 his3Δ200 leu2Δ1 pESC-URA(PSO2)*	This work
MBY877	*MATa ura3-52 lys2-801_amber ade2-101_ochre trp1Δ63 his3Δ200 leu2Δ1 pso2::TRP1 sgs1::NatMX*	This work
MBY878	*MATa ura3-52 lys2-801_amber ade2-101_ochre trp1Δ63 his3Δ200 leu2Δ1 hrq1::His3MX6 pso2::TRP1 sgs1::NatMX*	This work

1. Sikorski R.S. and Hieter P. A system of shuttle vectors and yeast host strains designed for efficient manipulation of DNA in *Saccharomyces cerevisiae*. *Genetics.* 1989; 122: 19-27.